

Topological Signal Processing on Quantum Computers for Higher-Order Network Analysis

Caesnan M. G. Leditto,^{1,*} Angus Southwell,² Behnam Tonekaboni,³
 Gregory A. L. White,^{1,4} Muhammad Usman,^{3,5,1} and Kavan Modi^{2,1,†}

¹*School of Physics and Astronomy, Monash University, Clayton, VIC 3168, Australia*

²*Quantum for New South Wales, Haymarket, NSW 2000, Australia*

³*Quantum Systems, Data61, CSIRO, Clayton, VIC 3168, Australia*

⁴*Dahlem Center for Complex Quantum Systems,
 Freie Universität Berlin, 14195 Berlin, Germany*

⁵*School of Physics, The University of Melbourne, Parkville, VIC 3052, Australia*

Predicting and analyzing global behaviour of complex systems is challenging due to the intricate nature of their component interactions. Recent work has started modelling complex systems using networks endowed with multiway interactions among nodes, known as higher-order networks. In this context, simplicial complexes are a class of higher-order networks that have received significant attention due to their topological structure and connections to Hodge theory. Topological signal processing (TSP) utilizes these connections to analyze and manipulate signals defined on non-Euclidean domains such as simplicial complexes. In this work, we present a general quantum algorithm for implementing filtering processes in TSP and describe its application to extracting network data based on the Hodge decomposition. We leverage pre-existing tools introduced in recent quantum algorithms for topological data analysis and combine them with spectral filtering techniques using the quantum singular value transformation framework. While this paper serves as a proof-of-concept, we obtain a super-polynomial improvement over the best known classical algorithms for TSP filtering processes, modulo some important caveats about encoding and retrieving the data from a quantum state. The proposed algorithm generalizes the applicability of tools from quantum topological data analysis to novel applications in analyzing high-dimensional complex systems.

I. INTRODUCTION

Recent work in the field of signal processing has focused on understanding signals that are defined on domains other than time or space. In particular, there has been considerable research on signals which are defined on graphs [1–3] or, more generally, higher-order networks [4, 5]. In the graph context, a ‘signal’ means a value attributed to a node on the graph, and the edges denote interactions between the elements (vertices) of the system. This value often comes from real-world observations of some (potentially dynamical) system. This includes a discrete 1D signal — such as time series data; 2D signals on a grid — such as colour values in an image; or, more generally, 2D signals on an arbitrary graph. Figure 1 (a)–(c) show illustrations of signals. Moving beyond graphs and pairwise interactions, higher-order networks — or *hypergraphs* — can be far more expressive in capturing the interactions of a given system [6–9]. In a hypergraph, edges may connect to an arbitrary number of vertices. Consequently, signals associated with topological objects on higher-order networks (such as the edges and hyperedges) can represent data which is inherently multi-party. In this work, we are particularly interested in categories similar to the last case, where a signal is more generally defined on the k -body interactions (depicted in the 3-body case by triangles in Figure 1(d)) in a

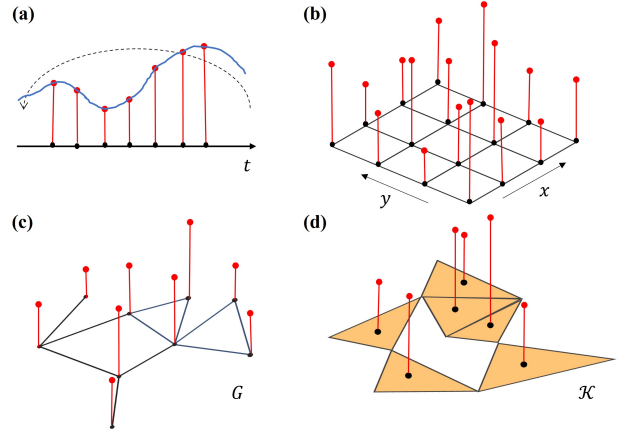


Figure 1. (a) discrete-time signals (1-D signals) with periodic boundary condition, (b) grid-like signals (2-D signals on $x - y$ plane), (c) node signals (signals on a graph G), and (d) simplicial signals (signals on a simplicial complex \mathcal{K}).

higher-order network. The topology of these higher-order interactions have a non-trivial impact on the evolution of many systems [10].

Equipped with this way of encoding data on vertices and (hyper)edges, graphs and networks can be utilized to study interactions captured in the signals between different elements of a system. The field of graph signal processing (GSP) leverages tools both from graph theory and signal processing to perform standard tasks with signals (such as denoising or filtering) on data defined over non-

* caesnan.leditto@monash.edu

† kavan.modi@transport.nsw.gov.au

Euclidean domains. GSP has been successfully applied to understand sensor networks [11], brain connectivity [12–14], protein interactions [15], and to perform image processing [16, 17]. However, just as graphs are insufficient to describe multi-way interactions, GSP is insufficient as a tool to study more complex systems. As a result, *topological* signal processing (TSP) has recently emerged as a method by which signals may be studied in the context of topological objects on higher-order networks. Already, these networks and the corresponding signals have been used to model an enormous variety of systems, such as the brain [18], research collaboration networks [19], and protein-protein interaction networks [20], where many-body interactions play vital roles in the dynamics of the underlying system. In this paper, we present a quantum algorithm for filtering and analyzing topological signals defined on a class of higher-order networks known as simplicial complexes. The theoretical complexity bounds of this algorithm show a promising advantage over the best currently known classical methods.

Higher-order networks are defined mathematically as a pair (\mathcal{V}, S) , where \mathcal{V} is the set of vertices (the individual elements being studied), and S is a set of subsets of \mathcal{V} describing the interactions between elements of \mathcal{V} . In a standard graph or network, S would be the edge set, a set of 2-element subsets of \mathcal{V} , whereas in higher-order networks S may contain larger subsets. Higher-order networks contain many rich sub-classes. In particular, we consider here the extensively-studied category of *simplicial complexes*. The defining property of a simplicial complex $\mathcal{K} = (\mathcal{V}, S)$ is that if we have some $A \subset S$, then every subset of A is also in S . Although this is not the most general hypergraph model, their extra structure allows for the use of tools from algebraic topology. This can be incredibly useful for analysing signals found on such complexes. Furthermore, many interesting physically and mathematically relevant systems can be represented by simplicial complexes. Hence, considering this class expands the available toolkit while maintaining versatility or applicability.

The use of simplicial complexes and algebraic topology in data analysis has an extensive history. Indeed, topological data analysis (TDA) [21–24] is an umbrella term for a wide range of statistical methods that employ techniques from algebraic topology to study real-world data. By analysing the shape of data from a topological viewpoint, TDA can both reduce data dimensionality and benefit from robustness to noise. These methods have seen wide-ranging applications, such as in sensor networks [25], financial market prediction [26], tumor classification [27], and analyzing collaboration networks characteristics [28]. A popular aspect of TDA is the study of *Betti numbers* of simplicial complexes. The Betti numbers $(\beta_k)_{k \geq 0}$ describe, at a high level, the number of k -dimensional “holes” in the simplicial complex, which in TDA is generated by the data set. These can be used for distinguishing data sets [29], for hypothesis testing [30], or as features for machine learning algorithms [31].

In tandem with the development of sophisticated classical data analysis algorithms, there has been an urgent need to showcase the utility of quantum computers in real-world cases. Consequently, there has been a proliferation of ideas in quantum data analysis and machine learning. In recent years, quantum algorithms for TDA (QTDA) have been proposed to efficiently compute the higher-order Betti numbers of simplicial complexes arising in applications of TDA [32–37]. The perceived advantage in contrast to classical algorithms is that the classical complexity of computing the k -th Betti number β_k of a simplicial complex has worst-case exponential scaling in k . This severely limits the capability to study the topology of higher-order interactions in networks using classical computers. On the other hand, since the seminal paper by Lloyd, Garnerone, and Zanardi [32], there has been a flurry of research about quantum algorithms for computing Betti numbers in fault-tolerant quantum computers. Although it was shown that Betti number estimation is QMA_1 -hard [33], one can relax the problem by approximating a normalized version of β_k . While in early years, there were several promising results indicating the potential for an exponential (in k) speedup over classical algorithms for estimating *approximate* normalized Betti numbers, recent results have tempered these expectations. In particular, Refs. [34, 37–39] have argued that the existence of a superpolynomial speedup over classical algorithms for this task is, at best, highly situational. In most cases, the quantum algorithms will provide a polynomial speedup compared to classical algorithms. Importantly, to overcome current quantum error correction overheads, it is highly desirable for this speedup to be greater than quadratic [40, 41].

a. Our contribution. In this paper, we adapt the tools used in QTDA to the new task of quantum topological signal processing (QTSP). In doing so, we introduce a broad range of new applications of quantum computers to the task of data analysis. The problem settings for QTSP and QTDA are quite different: QTDA works on point cloud data and defines sequences of simplicial complexes from that data (see an example given in Figure 6(a)), whereas QTSP is generally focused on studying signals on a fixed higher-order network (such as the example given in Figure 2(a)). Beyond this distinction, we can think of the QTSP as a generalization of QTDA that is applicable to a different range of tasks. QTDA involves projecting states to the kernel of the Hodge Laplacian \mathbf{L}_k (given formally in Definition 3) to determine its dimension (see Figure 6 as an illustration of the algorithm); in QTSP, we analyze the image of \mathbf{L}_k as well as the kernel (and thus the whole codomain) through the lens of what is known as the Hodge decomposition. Previous works in QTDA [36, 37, 39] often implement spectral filtering to construct a projection to the kernel $\ker(\mathbf{L}_k)$. The goal of QTSP is to, given a filtering task and some data, construct a quantum circuit that implements this filter on a quantum representation of the data (Figure 2(b)). Here, the quantum filter operator is designed to manipulate

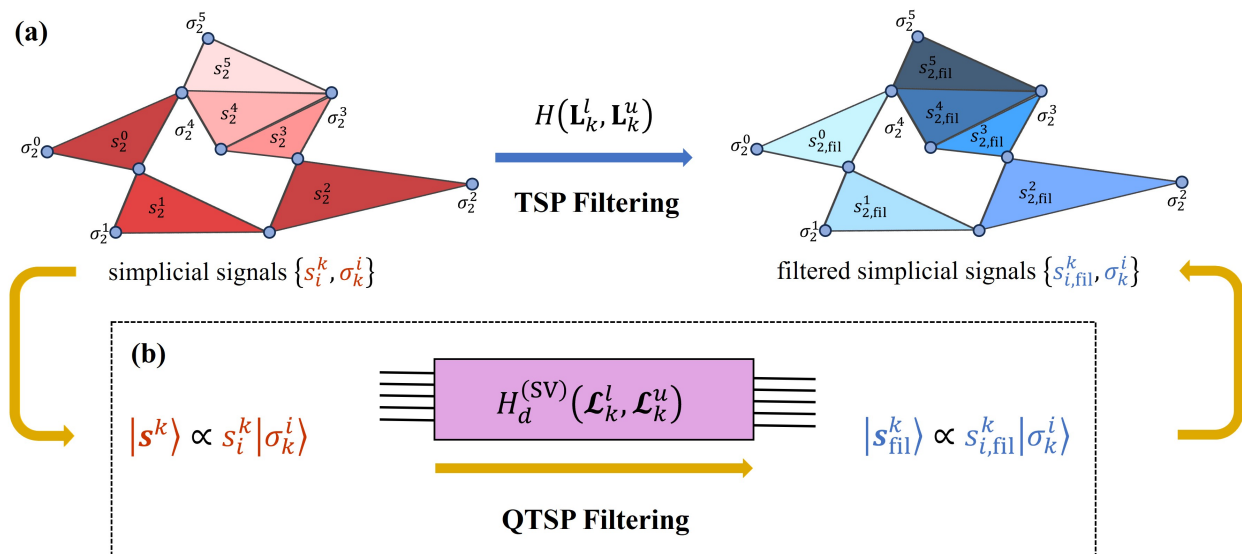


Figure 2. (a) A flowchart diagram for topological signal processing (TSP) filtering using a simplicial filter $H(\mathbf{L}_k^l, \mathbf{L}_k^u)$ with input simplicial signals $\{s_i^k\}$ defined on simplices $\{\sigma_k^i\}$ (with magnitudes represented by colour opacity) and the filtered simplicial signals $\{s_{i,fil}^k\}$. (b) A QTSP filtering process on a quantum computer using a quantum simplicial filter $H_d^{(SV)}(\mathcal{L}_k^l, \mathcal{L}_k^u)$ which filters a simplicial signal state $|s^k\rangle$, which encodes the signals $\{s_i^k\}$. The full pipeline of the algorithm is comprised of three subsequent subroutines: ENCODE, FILTER, and RETRIEVE, depicted by the flow of gold arrows.

not just the kernel of the Hodge Laplacian, but also its image. On the other hand, if the filter is just a projection to $\ker(\mathbf{L}_k)$, then we can recover the QTDA task of estimating Betti numbers as an application of QTSP.

We construct a quantum algorithm to efficiently perform TSP filtering on a fault-tolerant quantum computer. By efficiently, we mean that the complexity of our filtering algorithm scales polynomially in terms of the number of vertices, the dimension of the complex, and the order of the filter (formally defined in Section II). We also give a particular application of this general filtering algorithm. Modulo some caveats that we discuss later, the algorithm presented here is a promising avenue for a superpolynomial speedup over performing TSP on a classical computer, at least for some tasks. Here, we informally state our main result, which is given formally in Section III as Theorem 1.

Result 1. *We present a quantum algorithm for filtering topological signals defined on the k -dimensional simplices of a simplicial complex. If the simplicial complex is a clique complex, this algorithm scales linearly in k . In comparison, the complexity of performing the filtering on a classical computer scales exponentially in k .*

This theoretical speed-up comes with some important caveats and requires an in-depth technical justification before making any claims of a practical speed-up. In Section III we state the cost of implementing the filtering process (specifically in Theorem 1). We also discuss the hurdles that stand between our complexity results and a practical speed-up in performing an end-to-end implementation of our algorithm on (classical or quantum) data. Additionally, we showcase an application of

this result to extracting signal subcomponents based on Hodge decomposition, which we discuss in more detail in Sections II and III.

A brief background to topological signal processing and the specific description of the class of filtering tasks is given in Section II A. This class of tasks is very general, and given that higher-order networks of interest may contain thousands or millions of vertices, a superpolynomial advantage has huge potential. On the more cautioned side, signal processing on higher-order networks is a relatively new field, which means that concrete applications to test this quantum advantage in higher dimensions are not well understood. Our algorithm also only applies to clique complexes, a specific class of simplicial complexes defined by an underlying graph. Furthermore, this algorithm suffers the classic pitfalls of many quantum linear algebra (QLA) algorithms in data encoding and retrieval costs, and the costs of these steps may limit the speed-up in practice. Nonetheless, the generality of our framework lends itself to plenty of opportunity for a concrete quantum advantage to be achieved in the future.

b. Related works. Our work is the first to present a QTSP algorithm but it relies on several previous studies on QTDA and spectral filtering algorithms, which are based on quantum phase estimation algorithms. Quantum phase estimation has been used in many Hamiltonian simulation algorithms to showcase quantum advantages. Recently, quantum signal processing (QSP) [42, 43] and quantum singular value transformation (QSVT) [44] have provided new ways of implementing spectral filtering techniques. These techniques were exploited in Ref. [45] to construct minimax polynomial

filters that project states based on the corresponding known eigenvalues. Using this eigenstate filtering and the quantum Zeno effect, the authors presented a nearly optimal complexity for solving QLA problems. Such a filtering algorithm was employed in Ref. [46] to find the ground state below a given threshold. Notably, these QSVT-based filtering algorithms require classical computation costs to determine the rotation angles used in the circuit. Another filtering technique solely based on the linear combination of unitaries (LCU) method was given in Ref. [47], which avoids this heavy classical computation. As the Betti number estimation task can be viewed as finding the dimension of a ground-state subspace, Ref. [37] utilized this to construct a sequence of projections to the kernel of the Laplacian. Different filtering approaches have been used in Refs. [36, 39] to tackle a similar task using rectangular and Kaiser window filters. However, these methods gave polynomially worse scaling in time complexity compared to that of Ref. [37].

c. Organization. The remainder of the paper is laid out as follows. In Section II, we briefly overview the background mathematics and notations required. We also present the filtering problem in greater detail. Finally, in Section III, we state the main results of our paper and discuss the advantages and limitations of our algorithm. In Section IV, we discuss the precise details of our implementation and prove the necessary results about its complexity and correctness.

II. BACKGROUND OF THE SIMPLICIAL FILTER DESIGN PROBLEM

A. Simplicial homology

Topology has found practical applications across a huge range of domains, such as biology, computer science, quantum field theory, and statistics. This utility arises from the fact that both physical and abstract systems can be mapped onto topological spaces, enabling the adoption of topological approaches as an alternate analysis method. Simplicial complexes in particular have gained substantial attention as models that capture complex data representations or interactions, especially in the context of higher-order networks. Here, we provide a concise overview of simplicial homology and delve into essential tools commonly employed in the realms of TDA and TSP. For a more extensive discussion of these subjects, see Ref. [48].

We start from the notion of a simplicial complex, simplices, and their topological properties. Let $\mathcal{V} = \{v_1, \dots, v_n\}$ be a non-empty set called the vertex set. A simplicial complex \mathcal{K} is a set of subsets of \mathcal{V} with two properties: (a) \mathcal{K} contains all singleton subsets, that is, $\{v\} \in \mathcal{K}$ for all $v \in \mathcal{V}$; (b) if $\sigma \in \mathcal{K}$, then every subset of σ is also in \mathcal{K} . We say that σ is a k -simplex (short for k -dimensional simplex) when $|\sigma| = k + 1$. If $\sigma' \subset \sigma$ with $q + 1 < k + 1$ elements, then σ' is called a (q) -face of σ .

We focus on a particular class of simplicial complexes that piqued the interest of the quantum community working on TDA, which is the class of *clique complexes*. A clique complex is a simplicial complex whose structure is entirely determined by an underlying graph G . Formally, a clique complex $\mathcal{K} = \mathcal{K}(G)$ is a simplicial complex where a set $\{v_{i_0}, \dots, v_{i_k}\}$ is a k -simplex in \mathcal{K} if and only if $\{v_{i_0}, \dots, v_{i_k}\}$ is a $(k + 1)$ -clique (a set of $k + 1$ mutually adjacent vertices) in G . It is straightforward to see that this is a simplicial complex: each vertex forms a 1-clique on its own, and an induced subgraph of a clique is a clique. We focus on this class of complexes as their structure allows for efficient quantum circuit implementations of some otherwise difficult functions.

Modelling systems and their signals using simplicial complexes, instead of general hypergraphs, allows the use of tools from algebraic topology. In order to build the algebraic objects of interest later, one associates an orientation to each simplex in the complex. An orientation $\epsilon(\sigma)$ of a simplex σ is the parity of an ordering of the vertices ϵ (as an element of the permutation group S_n). Let $j \in [k + 1] := \{0, \dots, k\}$ and $i_j \in [n] := \{0, \dots, n - 1\}$. An orientation of a simplex $\sigma = \{v_{i_0}, \dots, v_{i_k}\}$ is an ordering of the vertices, which we denote $[v_{i_0}, \dots, v_{i_k}]$, where two orderings are equivalent if they differ by an even number of transpositions. Thus, there are only two distinct orientations for each simplex, often referred to as positive and negative.

One particular class of algebraic objects that mathematically underpins our work is the space of k -chains. These are defined as formal sums of simplices in the complex. For our purposes, the space of k -chains $\mathfrak{C}_k := \mathfrak{C}_k(\mathcal{K})$ of a simplicial complex \mathcal{K} is (isomorphic to) a real vector space where the basis is a collection of k -simplices in \mathcal{K} , i.e., $\mathfrak{C}_k := \{\sum_{i=0}^{n_k-1} c_i \sigma_k^i \mid c_i \in \mathbb{R}\}$, where n_k is the number of k -simplices in \mathcal{K} . The different spaces $\mathfrak{C}_k(\mathcal{K})$ associated with different dimensions k are related to each other by maps known as boundary operators. The k -th boundary operator $\partial_k : \mathfrak{C}_k \rightarrow \mathfrak{C}_{k-1}$ is a linear map such that for $\sigma_k = [v_{i_0}, \dots, v_{i_k}] \in \mathfrak{C}_k$,

$$\partial_k \sigma_k := \sum_{j=0}^k (-1)^j [v_{i_0}, \dots, v_{i_{j-1}}, v_{i_{j+1}}, \dots, v_{i_k}]. \quad (1)$$

In each summand, a different vertex v_{i_j} is removed from the simplex. That is, ∂_k maps a k -simplex to a formal sum of its $(k - 1)$ -faces, which are the boundary of the k -simplex in a topological sense. Since this map acts linearly on the space of k -chains, we can represent it by a matrix. Let \mathbf{B}_k be the matrix representation of ∂_k , using the canonical bases of k -simplices and $(k - 1)$ -simplices for $\mathfrak{C}_k(\mathcal{K})$ and $\mathfrak{C}_{k-1}(\mathcal{K})$ respectively. The entries of \mathbf{B}_k are

$$(\mathbf{B}_k)_{ij} = \begin{cases} 1, & \text{if } i \neq j, \sigma_{k-1}^i \subset \sigma_k^j, \epsilon(\sigma_{k-1}^i) \sim \epsilon(\sigma_k^j) \\ -1, & \text{if } i \neq j, \sigma_{k-1}^i \subset \sigma_k^j, \epsilon(\sigma_{k-1}^i) \approx \epsilon(\sigma_k^j) \\ 0, & \text{otherwise,} \end{cases} \quad (2)$$

where $\epsilon(\sigma_{k-1}^i) \sim \epsilon(\sigma_k^j)$ means σ_{k-1}^i and σ_k^j have the same orientation (both positive or both negative) and $\epsilon(\sigma_{k-1}^i) \approx \epsilon(\sigma_k^j)$ means σ_{k-1}^i and σ_k^j have different orientations [49]. Thus, the ± 1 entries account for the orientation of each k -simplex relative to its boundary $(k-1)$ -faces. In this paper, we generally refer to the boundary operator by its matrix representation \mathbf{B}_k .

The adjoint (equivalently, transpose) of the boundary operator \mathbf{B}_k^T is called the coboundary operator and naturally maps from \mathfrak{C}_{k-1} to \mathfrak{C}_k . The boundary and coboundary operators are used to construct the central object of our consideration: the Hodge Laplacian. The Hodge Laplacian matrix \mathbf{L}_k is defined as

$$\mathbf{L}_k := \begin{cases} \mathbf{B}_{k+1}\mathbf{B}_{k+1}^T, & \text{for } k = 0 \\ \mathbf{B}_k^T\mathbf{B}_k + \mathbf{B}_{k+1}\mathbf{B}_{k+1}^T, & \text{for } 1 < k < n - 2 \\ \mathbf{B}_k^T\mathbf{B}_k, & \text{for } k = n - 1 \end{cases} \quad (3)$$

where superscript T indicates the matrix transpose operation. Furthermore, the lower and upper Hodge Laplacian operators are defined as $\mathbf{L}_k^l := \mathbf{B}_k^T\mathbf{B}_k$ and $\mathbf{L}_k^u := \mathbf{B}_{k+1}\mathbf{B}_{k+1}^T$ respectively. Hence, the lower and upper Hodge Laplacians \mathbf{L}_k^l and \mathbf{L}_k^u are given by

$$\mathbf{L}_k^l = \begin{cases} \deg_l(\sigma_k^i), & \text{if } i = j \\ 1, & \text{if } i \neq j, \sigma_k^i \sim_l \sigma_k^j, \epsilon(\sigma_k^i) \sim \epsilon(\sigma_k^j) \\ -1, & \text{if } i \neq j, \sigma_k^i \sim_l \sigma_k^j, \epsilon(\sigma_k^i) \approx \epsilon(\sigma_k^j) \\ 0, & \text{otherwise,} \end{cases} \quad (4)$$

$$\mathbf{L}_k^u = \begin{cases} \deg_u(\sigma_k^i), & \text{if } i = j \\ 1, & \text{if } i \neq j, \sigma_k^i \sim_u \sigma_k^j, \epsilon(\sigma_k^i) \sim \epsilon(\sigma_k^j) \\ -1, & \text{if } i \neq j, \sigma_k^i \sim_u \sigma_k^j, \epsilon(\sigma_k^i) \approx \epsilon(\sigma_k^j) \\ 0, & \text{otherwise,} \end{cases} \quad (5)$$

where $\deg_l(\sigma_k^i)$ ($\deg_u(\sigma_k^i)$) means the number of $(k-1)$ -simplices ($(k+1)$ -simplices) which are faces of σ_k^i (which have σ_k^i as a face) [49]. The sign \sim_l is a relation between k -simplices sharing a $(k-1)$ -face, and \sim_u is a relation between faces of a $(k+1)$ -simplex. Remarkably, the definitions of \mathbf{L}_k^l and \mathbf{L}_k^u do not depend on the choice of orientation of the simplices in the complex. This operator \mathbf{L}_k and its constituent elements form the building blocks for the topological signal processing operations we examine in this paper. Note that \mathbf{L}_k , \mathbf{L}_k^l , and \mathbf{L}_k^u are all real, symmetric matrices.

The connection to TDA and Betti number estimation is through the Hodge Laplacian. Denote $\mathfrak{B}_k := \text{im}(\partial_{k+1}) \subseteq \mathfrak{C}_k$ and $\mathfrak{Z}_k := \ker(\partial_k) \subseteq \mathfrak{C}_k$. The k -th homology group of a simplicial complex \mathcal{K} is given by the quotient group $\mathfrak{H}_k := \frac{\mathfrak{B}_k}{\mathfrak{Z}_k}$. The dimension of this group $\dim(\mathfrak{H}_k)$ is the k -th Betti number β_k . Equivalently, in terms of the matrix representation, the k -th Betti number is equal to $\dim(\ker(\mathbf{L}_k))$. This is the basis of TDA

algorithms for counting Betti numbers, and captures how the tasks of TDA and TSP are related mathematically.

B. Topological signal processing (TSP)

Here we formally introduce the mathematical background to TSP. We use the language and terminology used by Barbarossa and Sardellitti [4] and also by Yang, Isufi, Schaub, and Leus [50], and refer interested readers to these papers for more details. The aim of signal processing is to modulate the various components — determined by some structured set of frequency ranges — of the signal. This requires the design of a *filter*: an operator with appropriate input-output relations to transform the signal into something more desirable. In general, the nature of such a filter will be specific to the task at hand. For example, in discrete-time signal processing, a typical filtering task is suppressing high frequency noise. Denoising is achieved by utilising a shift operator and attenuating higher frequency components of the signal by weighting the signal in the frequency domain using the eigenvalues of the shift operator. In the framework of topological signal processing, the Hodge Laplacian \mathbf{L}_k plays the role of the shift operator.

The formalism and topological properties of a simplicial signal defined on a simplicial complex are as follows. Let \mathcal{K} be a simplicial complex with n_k k -simplices. A *simplicial signal* is a k -cochain, which is a linear functional $s^k : \mathfrak{C}_k(\mathcal{K}) \rightarrow \mathbb{R}$. This definition of a simplicial signal is equivalent to assigning a value $c_i \in \mathbb{R}$ to each k -simplex $\sigma_k^i \in \mathcal{K}$ for all $i \in [n_k]$. Since the space of k -cochains is an n_k -dimensional vector space over \mathbb{R} (where n_k is the number of k -simplices in \mathcal{K}), this gives rise to an isomorphism between \mathfrak{C}_k and \mathbb{R}^{n_k} . Therefore, we can represent the simplicial signal by a vector $\mathbf{s}^k \in \mathbb{R}^{n_k}$. In this language, the i -th entry of the signal vector is simply the signal associated with the i -th simplex, for some ordering of the simplices. For example, a simplicial complex could describe the collaboration network of researchers, where a set of researchers form a simplex if they all have a joint publication. A natural k -simplicial signal on this network would be the number of joint publications of each group of $k+1$ authors, which can be considered as a vector.

The vector space \mathbb{R}^{n_k} can be represented as the direct sum of three orthogonal subspaces defined in terms of the boundary maps and the Laplacian. This is known as the *Hodge decomposition*, which states that

$$\mathbb{R}^{n_k} = \ker(\mathbf{L}_k) \oplus \text{im}(\mathbf{B}_k^T) \oplus \text{im}(\mathbf{B}_{k+1}).$$

The three subspaces $\ker(\mathbf{L}_k)$, $\text{im}(\mathbf{B}_k^T)$, and $\text{im}(\mathbf{B}_{k+1})$ are known in TSP literature as the *harmonic*, *gradient*, and *curl* subspaces, respectively. These names are drawn from the analogously named Helmholtz-Hodge decomposition in the context of discrete vector fields, which is a special case of the Hodge decomposition for edge signals (i.e. the case $k=1$). Since \mathbf{L}_k is a Hermitian matrix, the

eigenvectors of \mathbf{L}_k can be used to construct an orthonormal basis of \mathbb{R}^{n_k} . Each eigenvector belongs to precisely one of these orthogonal spaces. Thus, each $\mathbf{s}^k \in \mathbb{R}^{n_k}$ can be decomposed into three orthogonal components

$$\mathbf{s}^k := \mathbf{s}_H^k + \mathbf{s}_G^k + \mathbf{s}_C^k, \quad (6)$$

where $\mathbf{s}_H^k \in \ker(\mathbf{L}_k)$, $\mathbf{s}_G^k \in \text{im}(\mathbf{B}_k^T)$, and $\mathbf{s}_C^k \in \text{im}(\mathbf{B}_{k+1})$. The orthogonality of these components allows them to be modulated somewhat independently by applying functions to the eigenvalues of the eigenvectors of the respective spaces.

Incorporating signal processing terminology from discrete-time signals, a notion of ‘‘frequency’’ of a simplicial signal has been defined that relates to the eigenvalues of \mathbf{L}_k . Let $\mathbf{L}_k = \mathbf{U}\mathbf{\Lambda}_k\mathbf{U}^T$ be an eigendecomposition of the Hodge Laplacian, where $\mathbf{\Lambda}_k$ is a diagonal matrix where $(\mathbf{\Lambda}_k)_{ii} = \lambda_{k,i}$ is an eigenvalue of \mathbf{L}_k for each $i \in [n_k]$, and \mathbf{U} is a unitary matrix composed of the eigenvectors of \mathbf{L}_k in the chosen basis. Then the *simplicial Fourier transform* is defined as $\tilde{\mathbf{s}}_k := \mathbf{U}^T \mathbf{s}_k$. This paves the way for implementing a filtering process analogous to discrete-time signal processing by modulating the so-called frequencies.

The standard definition of a *simplicial filter* follows from exploring this connection between discrete signals and the Hodge Laplacian. As the graph Laplacian $\mathbf{L}_0 := \mathbf{L}_G$ plays the role of filter operator primitive in GSP, the Hodge Laplacian \mathbf{L}_k has similar functionality in TSP. This filter is a map from the space of k -cochains to itself. Keeping in mind the aforementioned isomorphism to \mathbb{R}^{n_k} , this can be considered as a map from \mathbb{R}^{n_k} to itself. Consequently, a filter is defined by its action on the basis of eigenvectors of the Hodge Laplacian, which is equivalent to defining a function $g: \mathbb{R} \rightarrow \mathbb{R}$ by its action on the eigenvalues $\{\lambda_{k,i}\}$ of \mathbf{L}_k . Let us first define

$$\begin{aligned} \text{Eig}^H(\mathbf{L}_k) &:= \{\lambda_{k,i}^H\}_{i \in [n_k^H]}, \quad \text{Eig}^G(\mathbf{L}_k) := \{\lambda_{k,i}^G\}_{i \in [n_k^G]}, \\ \text{Eig}^C(\mathbf{L}_k) &:= \{\lambda_{k,i}^C\}_{i \in [n_k^C]} \end{aligned}$$

to be the sets of harmonic, gradient, and curl eigenvalues of \mathbf{L}_k respectively, where n_k^H , n_k^G , and n_k^C are the numbers of eigenvalues in each set. We denote by $\mathbf{0}_k^H$ a square matrix with all zero entries with size equal to the dimension of $\ker(\mathbf{L}_k)$. It follows from the Hodge decomposition that $\mathbf{\Lambda}_k = \mathbf{0}_k^H \oplus \mathbf{\Lambda}_k^G \oplus \mathbf{\Lambda}_k^C$, where $\mathbf{\Lambda}_k^G$ and $\mathbf{\Lambda}_k^C$ denote diagonal matrices with entries $(\mathbf{\Lambda}_k^G)_{ii} = \lambda_{k,i}^G$ for all $i \in [n_k^G]$ and $(\mathbf{\Lambda}_k^C)_{ii} = \lambda_{k,i}^C$ for all $i \in [n_k^C]$.

Due to the decomposition $\mathbf{L}_k = \mathbf{L}_k^\ell + \mathbf{L}_k^u$ of the Hodge Laplacian into lower and upper Laplacians, the Hodge Laplacian performs shift-and-sum operations in two different manners. Specifically, simplicial signals can be subjected to shifting and summation based on both \mathbf{L}_k^ℓ and \mathbf{L}_k^u , which shift signals across lower and upper adjacencies respectively. Thus, a comprehensive simplicial filter should accommodate shift operations in both di-

rections. The definition of a filter given below, commonly used in TSP literature (see e.g. [51]), encapsulates this generality. A simplicial filter of order d is a multivariate polynomial of total degree $d := \max\{d_\ell, d_u\}$, $H(\mathbf{L}_k^\ell, \mathbf{L}_k^u): \mathbb{R}^{n_k} \rightarrow \mathbb{R}^{n_k}$, defined as

$$H(\mathbf{L}_k^\ell, \mathbf{L}_k^u) := h_0 \mathbf{I} + \sum_{i_\ell=1}^{d_\ell} h_{i_\ell}^\ell (\mathbf{L}_k^\ell)^{i_\ell} + \sum_{i_u=1}^{d_u} h_{i_u}^u (\mathbf{L}_k^u)^{i_u} \quad (7)$$

where $h_0, h_{i_\ell}^\ell, h_{i_u}^u \in \mathbb{R}$ are called the simplicial filter coefficients. Alternatively, some papers in TSP [50, 52] define a simplified version of this filter, which is given by a degree- d real-valued polynomial of the Hodge Laplacian

$$H(\mathbf{L}_k) = \sum_{i=0}^d h_i (\mathbf{L}_k)^i, \quad (8)$$

where $h_i \in \mathbb{R}$. This is accommodated in Eq. (7) by setting $h_i^\ell = h_i^u$ for all $i \leq d$. However, the simplified version of the simplicial filter is less expressive and less able to distinguish signals from the different subspaces described by the Hodge decomposition. Hence, for certain tasks (such as extracting the signal subcomponents \mathbf{s}_H^k , \mathbf{s}_G^k , and \mathbf{s}_C^k given in Eq. (6)), $H(\mathbf{L}_k)$ does not give accurate filtered signals. Therefore, we focus on the type of simplicial filter defined in Eq. (7).

If one has access to an eigendecomposition of \mathbf{L}_k , then the filter can be expressed as $H(\mathbf{L}_k^\ell, \mathbf{L}_k^u) = \mathbf{U}\tilde{H}(\mathbf{\Lambda}_k)\mathbf{U}^T$, where \tilde{H} is called the *filter frequency response* of $H(\mathbf{L}_k^\ell, \mathbf{L}_k^u)$. If we decompose $\tilde{H}(\mathbf{\Lambda}_k)$ into its harmonic, gradient, and curl parts, this can be written as $\tilde{H} = \tilde{H}^H \oplus \tilde{H}^G \oplus \tilde{H}^C$, where

$$\begin{aligned} \tilde{H}^H(\mathbf{\Lambda}_k^H) &= h_0 \mathbf{I}, \\ \tilde{H}^G(\mathbf{\Lambda}_k^G) &= h_0 \mathbf{I} + \sum_{i_\ell=1}^{d_\ell} h_{i_\ell}^\ell (\mathbf{\Lambda}_k^G)^{i_\ell}, \\ \tilde{H}^C(\mathbf{\Lambda}_k^C) &= h_0 \mathbf{I} + \sum_{i_u=1}^{d_u} h_{i_u}^u (\mathbf{\Lambda}_k^C)^{i_u}. \end{aligned} \quad (9)$$

Having defined the filter frequency response of a simplicial filter, one can now describe the filter design problem, which is central to the field of topological signal processing.

Problem 1 (Simplicial Filter Design Problem [50, 51]). *Given desired frequency responses $g^H(x)$, $g^G(x)$, $g^C(x)$ for all x in $\text{Eig}^H(\mathbf{L}_k)$, $\text{Eig}^G(\mathbf{L}_k)$, $\text{Eig}^C(\mathbf{L}_k)$ respectively, and $\delta_{g^H}, \delta_{g^G}, \delta_{g^C} \in \mathbb{R}_+$, the filter design problem is the task of finding $\tilde{H}(\mathbf{\Lambda}_k)$ (accordingly $H(\mathbf{L}_k^\ell, \mathbf{L}_k^u)$) such that*

$$\begin{aligned} \left\| g^H(x) - \tilde{H}^H(x) \right\| &\leq \delta_{g^H}, \quad \text{for all } x \in \text{Eig}^H(\mathbf{L}_k), \\ \left\| g^G(x) - \tilde{H}^G(x) \right\| &\leq \delta_{g^G}, \quad \text{for all } x \in \text{Eig}^G(\mathbf{L}_k), \\ \left\| g^C(x) - \tilde{H}^C(x) \right\| &\leq \delta_{g^C}, \quad \text{for all } x \in \text{Eig}^C(\mathbf{L}_k). \end{aligned} \quad (10)$$

As the polynomials are characterized by their coefficients, the above problem can be translated to the problem of finding the simplicial filter coefficients $\{h_0, \{h_{i_\ell}\}_{i_\ell \in [d_\ell]}, \{h_{i_u}\}_{i_u \in [d_u]}\}$ that construct polynomials satisfying the above conditions.

Simplicial filter design problems can be solved by solving least square problems. However, this method requires explicit knowledge of the eigenvalues of \mathbf{L}_k and suffers from numerical instability [51]. In practice, eigen-decompositions are computationally expensive, so other methods are used to determine the precise filter coefficients for a desired frequency response. One approach that alleviates such issues is known as the Chebyshev filter design [51]. In this approach, the functions g^G, g^C are assumed to be continuous functions with domains $[0, \lambda_{k,\max}^G]$ and $[0, \lambda_{k,\max}^C]$ respectively. These functions are then approximated using a series of Chebyshev polynomials. Since the gradient and curl frequency responses affect the harmonic subspace, it is required that $g^G(0) = g^C(0) = \mathbf{c}_0$ (for some constant \mathbf{c}_0) to ensure the correct response on the harmonic subspace (i.e., $\tilde{H}^H(x) = \mathbf{c}_0$). Let T_i be the i -th Chebyshev polynomial of the first kind. Then the Chebyshev filter [51] is defined as

$$H_{\text{Cheb}}(\mathbf{L}_k^\ell, \mathbf{L}_k^u) := \sum_{i=0}^{d_\ell} \mathbf{c}_i^\ell T_i \left(\frac{2\mathbf{L}_k^\ell - \mathbf{I}}{\lambda_{G,\max}} - \mathbf{I} \right) + \sum_{i=0}^{d_u} \mathbf{c}_i^u T_i \left(\frac{2\mathbf{L}_k^u}{\lambda_{C,\max}} - \mathbf{I} \right) - \mathbf{c}_0 \mathbf{I}, \quad (11)$$

where $g^G(x) \approx \sum_{i_\ell=0}^{d_\ell} \mathbf{c}_{i_\ell}^\ell T_{i_\ell}(x)$ and $g^C(x) \approx \sum_{i_u=0}^{d_u} \mathbf{c}_{i_u}^u T_{i_u}(x)$ for all $x \in [0, 1]$ and $\lambda_{G,\max}, \lambda_{C,\max}$ are the maximum eigenvalues of \mathbf{L}_k^ℓ and \mathbf{L}_k^u respectively. The Chebyshev filter is characterized by its coefficients $\{\mathbf{c}_0, \{\mathbf{c}_{i_\ell}^\ell\}_{i_\ell \in [d_\ell+1]}, \{\mathbf{c}_{i_u}^u\}_{i_u \in [d_u+1]}\}$, called the Chebyshev filter coefficients. The advantages of this design are two-fold. Firstly, it avoids directly computing all of the eigenvalues of \mathbf{L}_k , which is expensive (even the largest eigenvalues of \mathbf{L}_k^ℓ and \mathbf{L}_k^u can be bounded from above rather than explicitly computed). Secondly, this framework allows for the filtering algorithm to be implemented distributively in the classical setting. The latter can significantly reduce the classical computational burden for local computation, albeit at the expense of having exponentially many networked computers [51, 53].

Generally, the filtering operation is computationally challenging in higher-order network analysis. In standard implementations [50, 51], the computational complexity grows linearly in the number of multi-way interactions captured in the higher-order network. In real-world scenarios, these large higher-order interactions, modelled in higher-dimensional simplices, have been detected in collaboration [52, 54], social [55], and brain networks [18]. Explicitly, the number of possible k -wise interactions, given by $\binom{n}{k}$, grows exponentially in k (for the practically relevant ranges of k), and thus the number of possible higher-order interactions in these large networks is enor-

mous. To combat this exponential relationship between the dimension of the simplicial complex and the classical complexity, we aim to reduce the TSP filtering cost by utilizing quantum computers. In the following subsection, we re-express the simplicial filter design problem in Problem 1, as well as the filtering process, in the quantum linear algebra framework and briefly describe how we modify tools from QTDA to implement a quantum analogue of the filtering operation on quantum computers. Then, we give our main results on the complexity of this implementation in Section III.

C. Quantum linear algebra

Both QTDA and QTSP can be considered as part of the class of quantum linear algebra (QLA) algorithms. QLA constitutes a broad church of quantum algorithms with perceived applications in machine learning and data analysis. The breakthrough of quantum algorithms for linear algebra problems started from the seminal work by Harrow, Hassidim, and Lloyd [56] that, given a Hermitian matrix \mathbf{A} and a (state) vector $|\mathbf{v}_{\text{in}}\rangle$, used quantum phase estimation and Hamiltonian simulation to prepare a state $|\tilde{\mathbf{v}}_{\text{sol}}\rangle$, an approximate solution to $\mathbf{A}|\mathbf{v}_{\text{sol}}\rangle = |\mathbf{v}_{\text{in}}\rangle$. Since then, QLA concepts have been applied to a wide range of topics in big data analysis and machine learning, including support vector machines [57], principle component analysis [58], recommendation systems [59], and clustering [60, 61].

However, as pointed out by Aaronson [62], even under the favourable assumptions that there exist efficient algorithms that encode $|\mathbf{v}_{\text{in}}\rangle$ and \mathbf{A} in a quantum circuit, many QLA algorithms such as the HHL algorithm only “solve” the desired linear algebra problem efficiently in the sense that they can rapidly prepare a quantum state $|\tilde{\mathbf{v}}_{\text{sol}}\rangle$, a quantum state representing an approximation of \mathbf{v}_{sol} . At this point, tomography must be performed to retrieve the information encoded in $|\tilde{\mathbf{v}}_{\text{sol}}\rangle$ to obtain the solution. This brings additional costs and sources of error. Thus, the whole pipeline of QLA, including the step to obtain a (classical) description of a state $|\tilde{\mathbf{v}}_{\text{sol}}\rangle$ which approximates the state $|\mathbf{v}_{\text{sol}}\rangle$, can be described as follows.

1. A classical data INPUT_c is given in the form of a list of vector components $\{v_{\text{in}}^i\}$ of a data vector \mathbf{v}_{in} and a list of entries $\{A_{ij}\}$ of a matrix \mathbf{A} that implements a linear transformation to $\{v_{\text{in}}^i\}$. Given a TASK to solve or accomplish and a vector \mathbf{v}_{in} , one can obtain the solution to the TASK, \mathbf{v}_{sol} , by employing a classical algorithm $\text{ALG}_c(\mathbf{A})$.
2. In ENCODE step, the set of vector components $\{v_{\text{in}}^i\}$ is encoded in the quantum state $|\mathbf{v}_{\text{in}}\rangle$, either in the amplitudes, basis states, or both, creating the input state $\text{INPUT}_q := \{|\mathbf{v}_{\text{in}}\rangle\}$.
3. A quantum algorithm ALG_q starts by encoding the matrix \mathbf{A} (or an approximation of \mathbf{A}) as a unitary

operator \mathbf{U}_A that is implementable in a quantum circuit. Then, it takes INPUT_q to solve the TASK by transforming $|\mathbf{v}_{\text{in}}\rangle \mapsto |\tilde{\mathbf{v}}_{\text{sol}}\rangle := \text{ALG}_q(\mathbf{U}_A)|\mathbf{v}_{\text{in}}\rangle$ such that $\| |\mathbf{v}_{\text{sol}}\rangle - |\tilde{\mathbf{v}}_{\text{sol}}\rangle \| \leq \delta$, where δ is an error from approximating the solution. In other words, $\text{OUTPUT}_q := |\tilde{\mathbf{v}}_{\text{sol}}\rangle$ is the approximate solution to the TASK.

4. An additional RETRIEVE step is required in order to obtain classical information about the approximate solution encoded in $|\tilde{\mathbf{v}}_{\text{sol}}\rangle$. This step normally consists of some variant of state tomography. From this one obtains a classical description of an approximation $|\hat{\mathbf{v}}_{\text{sol}}\rangle$ to $|\mathbf{v}_{\text{sol}}\rangle$, which carries an additional error ε such that $\| |\hat{\mathbf{v}}_{\text{sol}}\rangle - |\tilde{\mathbf{v}}_{\text{sol}}\rangle \| \leq \varepsilon$. As a result, one has $\| |\mathbf{v}_{\text{sol}}\rangle - |\hat{\mathbf{v}}_{\text{sol}}\rangle \| \leq \delta + \varepsilon$.

Our algorithm for TSP filtering on quantum computers fits into this QLA paradigm. We describe how to encode the simplicial signals in a quantum state $|\mathbf{v}_{\text{in}}\rangle = |\mathbf{s}^k\rangle$ and build a circuit that has the action of a polynomial of the lower and upper Laplacians on the subspace containing $|\mathbf{s}^k\rangle$. Due to nuances in implementing the quantum algorithm, the filters we implement are inspired by but distinct from the Chebyshev filter design. In our case, the upper and lower Laplacian are each rescaled such that their eigenvalues are in $[0, 1]$ so that they can be embedded in unitary matrices. In kind, we assume that $g^G, g^C : [0, 1] \rightarrow [-1, 1]$. We discuss this in more detail in the following section.

III. A QUANTUM IMPLEMENTATION OF TOPOLOGICAL SIGNAL PROCESSING

In this section we formally state our main result, where we give a general framework for implementing simplicial filters on fault-tolerant quantum computers. In TSP, a solution to Problem 1 connects the desired frequency responses $\{g^H, g^G, g^C\}$ with a set of polynomial coefficients. The filtering algorithm then aims to output a filtered simplicial signal given input simplicial signal data \mathbf{s}^k and the filter as described in Eq. (7). In order to make the problem more amenable to implementation on a quantum computer, we focus on a subset of filtering problems inspired by the Chebyshev filter design, originally defined in Refs. [50, 51] and given here in Eq. (11). We require that the frequency responses g^G and g^C are continuous. More strictly than this, we will assume that these functions are (approximated by) polynomials. As the eigenvalues of any operator embedded in a unitary matrix are bounded by 1 and $\mathbf{L}_k^\ell, \mathbf{L}_k^u$ are Hermitian, we impose that $g^G, g^C : [0, 1] \rightarrow [-1, 1]$. We also rescale the upper and lower Hodge Laplacians such that their eigenvalues are bounded by 1. This is similar but not identical to the rescaling present in the Chebyshev filter design. We also impose that $g^G(0) = g^C(0) = g^H = \mathfrak{h}_0$ for some real constant $\mathfrak{h}_0 \in [0, 1]$. Given a set of continuous frequency

responses satisfying these properties, we present an algorithm for performing the TSP filtering operation on a fault-tolerant quantum computer. The precise details of the filter are given in Eq. (12). This section gives an overview of this quantum algorithm and of its properties. Then, we give the specifics and detailed analysis of the algorithm in Section IV.

This quantum topological signal processing (QTSP) filtering algorithm leverages the construction and use of the Hodge Laplacian operator introduced in previous QTDA literature [35, 37, 39]. Although quantum spectral filtering techniques [45, 46] using a polynomial of the Hodge Laplacian have been used recently in Refs. [36, 37, 39] for estimating Betti numbers, the implementation of such techniques in more general cases remains unexplored. The framework wherein the QTDA algorithm exhibits a polynomial speed up over classical TDA is challenging to identify in real-world scenarios [39]. Hence, our focus centres on adapting tools used in the QTDA algorithm for filtering purposes within the TSP framework. This broadens the scope of these tools to higher-order network analysis, with the aim of increasing the likelihood of finding a practical quantum advantage. Below we sketch a high-level picture of our QTSP algorithm (presented in the QLA structure outlined in Section II).

1. Classical data representing a topological signal $\mathbf{s}^k \in \mathbb{R}^{n_k}$ is given in the form of a list of signal values s_i^k for each k -simplex σ_k^i . The frequency responses are functions $g^G, g^C : [0, 1] \rightarrow [-1, 1]$ such that $g^G(0) = g^C(0) = g^H = \mathfrak{h}_0$ for some real constant $\mathfrak{h}_0 \in [0, 1]$. We assume g^G and g^C are approximated by polynomials with coefficients $\{\mathfrak{h}_{i_\ell}^\ell\}_{i_\ell \in [d_\ell+1]}$ and $\{\mathfrak{h}_{i_u}^u\}_{i_u \in [d_u+1]}$ respectively. Hence, a classical input is defined as

$$\text{INPUT}_c := \left\{ \{s_i^k, \sigma_k^i\}, \{\mathfrak{h}_0, \mathfrak{h}_{i_\ell}^\ell, \mathfrak{h}_{i_u}^u\} \right\},$$

for $i \in [n_k], i_\ell \in [d_\ell + 1], i_u \in [d_u + 1]$.

2. The ENCODE step takes input $\{\{s_i^k, \sigma_k^i\}\} \in \text{INPUT}_c$ and a state $|\bar{0}\rangle$ and outputs the state $|\mathbf{s}^k\rangle$, which we call the *simplicial signal state* (defined formally in Section IV A). The simplices are encoded in the basis states in the simplicial signal state, and the corresponding signal values are encoded in the amplitudes. We consider two approaches to this, which, following the conventions of Ref. [37], are called the *compact* and *direct* approaches. In this paper we assume that this state is prepared by an oracle.
3. The FILTER step implements a polynomial of the upper and lower Hodge Laplacian defined by the classically-given filter coefficients $\{\mathfrak{h}_0, \mathfrak{h}_{i_\ell}^\ell, \mathfrak{h}_{i_u}^u\}$. We implement projected unitary encodings (PUEs, defined in Appendix A) of \mathbf{B}_k and \mathbf{B}_{k+1}^\dagger , the boundary operator and its adjoint with rescaling factors $\alpha_k, \alpha_{k+1} \in \mathbb{R}_+$ ($\alpha_k = \sqrt{n}$ in the direct approach and $\alpha_k = \sqrt{(n+1)(k+1)}$ in the compact approach). Then, using the quantum singular value

transformation (QSVT), we implement polynomial transformations of these operators. Specifically, we implement

$$\begin{aligned} h^G \left(\frac{\mathbf{B}_k}{\alpha_k} \right) &:= (g^G \circ f) \left(\frac{\mathbf{B}_k}{\alpha_k} \right) \\ &= \sum_{i_\ell=0}^{d_\ell} \mathfrak{h}_{i_\ell}^\ell \left(\frac{\mathbf{B}_k}{\alpha_k} \right)^{2i_\ell}, \\ h^C \left(\frac{\mathbf{B}_{k+1}^\dagger}{\alpha_{k+1}} \right) &:= (g^C \circ f) \left(\frac{\mathbf{B}_{k+1}^\dagger}{\alpha_{k+1}} \right) \\ &= \sum_{i_u=0}^{d_u} \mathfrak{h}_{i_u}^u \left(\frac{\mathbf{B}_{k+1}^\dagger}{\alpha_{k+1}} \right)^{2i_u}, \text{ and} \\ h^G(\mathbf{0}) &= h^C(\mathbf{0}) = \mathfrak{h}_0 \mathbf{I}, \end{aligned}$$

where $f(x) := x^2$. Note that $f(\mathbf{B}_k) = \mathbf{B}_k^\dagger \mathbf{B}_k = \mathbf{L}_k^\ell$ and $f(\mathbf{B}_{k+1}^\dagger) = \mathbf{B}_{k+1} \mathbf{B}_{k+1}^\dagger = \mathbf{L}_k^u$. We then use a linear combination of unitaries (LCU) to obtain a PUE of a *quantum simplicial filter of order $d = \max\{d_\ell, d_u\}$* , $H_d^{(\text{SV})} \left(\mathbf{L}_k^\ell / \alpha_k^2, \mathbf{L}_k^u / \alpha_{k+1}^2 \right)$, defined as

$$\begin{aligned} H_d^{(\text{SV})} \left(\frac{\mathbf{L}_k^\ell}{\alpha_k^2}, \frac{\mathbf{L}_k^u}{\alpha_{k+1}^2} \right) &:= \sum_{i_\ell=0}^{d_\ell} \mathfrak{h}_{i_\ell}^\ell \left(\frac{\mathbf{L}_k^\ell}{\alpha_k^2} \right)^{i_\ell} \\ &\quad + \sum_{i_u=0}^{d_u} \mathfrak{h}_{i_u}^u \left(\frac{\mathbf{L}_k^u}{\alpha_{k+1}^2} \right)^{i_u} - \mathfrak{h}_0 \mathbf{I}, \end{aligned} \quad (12)$$

4. In the RETRIEVE step, post-selection in ancilla qubit register is required to obtain the state $|\mathbf{s}_{\text{fil}}^k\rangle := H_d^{(\text{SV})} \left(\mathbf{L}_k^\ell / \alpha_k^2, \mathbf{L}_k^u / \alpha_{k+1}^2 \right) |\mathbf{s}^k\rangle$, the encoding of the filtered signal. Therefore, to boost the success probability of $|\mathbf{s}_{\text{fil}}^k\rangle$, the subsequent amplitude amplification technique is necessary. Afterwards, state tomography is used to obtain an approximation $\hat{\mathbf{s}}_{\text{fil}}^k$ to the filtered signal encoded in amplitudes of $|\mathbf{s}_{\text{fil}}^k\rangle$.

Put this way, the QTSP filtering process is simply a state preparation protocol for outputting $|\mathbf{s}_{\text{fil}}^k\rangle$ given the PUE of a quantum simplicial filter and the signal state $|\mathbf{s}^k\rangle$. Now we formally state our main result, which we call QTSP filtering, as follows.

Theorem 1 (QTSP filtering). *Let G be the underlying n -vertex graph of a clique complex $\mathcal{K}(G)$, and let $d = \max\{d_\ell, d_u\}$ be the order of the simplicial filter $H_d^{(\text{SV})}$ as given in Equation (12). There exists a quantum circuit implementing FILTER in*

- (a) (**Direct approach**) $O(dn \log n)$ time and $O(n)$ space;
- (b) (**Compact approach**) $O(dkn^2 \log(n) \log(\log(n)))$ time and $O(k \log n)$ space.

The proof of this theorem is given in Sec. IV C.

The time complexity of the non-parallel (or non-distributed) classical TSP algorithm given in Ref. [50] is $O(dn_k D)$, where n_k is the number of k -simplices in the complex and D is the maximum degree of a simplex in the complex (equivalently, the maximum number of non-zero, off-diagonal entries in a row of \mathbf{L}_k). An n -vertex simplicial complex may have as many as $\binom{n}{k+1}$ k -simplices and thus, the classical filtering complexity scales exponentially in k in the worst case. In comparison, our QTSP filtering algorithm scales polynomially in k . This suggests that QTSP filtering could be a promising avenue for achieving a super-quadratic speedup over performing TSP filtering on a classical computer.

However, there are some notable caveats to any claims of a practical speedup. Theorem 1 only accounts for the complexity of the PUE of $H_d^{(\text{SV})}(\mathbf{L}_k^\ell / \alpha_k^2, \mathbf{L}_k^u / \alpha_{k+1}^2)$, that is, the complexity of the FILTER step. In order to recover the filtered signal $|\mathbf{s}_{\text{fil}}^k\rangle$ one still needs to perform post-selection. In this work, we do not account for the complexity of this or any related amplitude amplification. We also do not consider the costs of creating the quantum state $|\mathbf{s}^k\rangle$ or recovering the desired information from $|\mathbf{s}_{\text{fil}}^k\rangle$ (i.e., the ENCODE or RETRIEVE steps). Some forms of data (such as a signal concentrated entirely on a single simplex) are computationally straightforward to encode in a quantum state. However, even in general it is worth noting that the space complexity of efficient state preparation methods (such as the one given by Zhang, Li, and Yuan [63]) have an ancilla cost comparable to the number of bits needed to store the vector on a classical computer. In terms of retrieving the filtered signal, the tomography methods of van Apeldoorn, Cornelissen, Gilyén, and Nannicini [64] allow for efficient ℓ_∞ -norm approximations of $|\mathbf{s}_{\text{fil}}^k\rangle$ to be obtained. This is particularly useful if a small number of amplitudes are expected to be large in the filtered signal. On the other hand, the output from the QTSP algorithm could potentially be used as the input for another quantum algorithm, such as a clustering algorithm, sidestepping the need for tomography on the signal state itself.

We also note that the scaling factors of α_k and α_{k+1} in Eq. (12) are not present in Eqs. (7) or (11). Thus, in order to make a precise comparison between the complexities of quantum and classical TSP for the same task, the filter coefficients for the quantum filter need to be adjusted to account for this rescaling. In comparison to the Chebyshev filter design, the rescaling factor given in Eq. (11) is roughly $\lambda_{G, \max}/2, \lambda_{C, \max}/2 = O(n)$ [65]. Thus, for simplicial complexes with a large maximum eigenvalue, the rescaling factors inherent in this design are similar to the rescaling factors in the quantum simplicial filters. The specifics of these rescalings, as well as encoding and retrieval costs, can vary greatly between applications; thus, we do not compare the complexities between classical and quantum algorithms for general simplicial filters. However, the broad range of possible applications of TSP increases the likelihood that there exist applications for

which these hurdles can be overcome, and a practical speed-up can be obtained.

We give a specific application of Theorem 1 related to the Hodge decomposition. This decomposition plays an important role in many areas ranging from analysis of biological networks to computer vision [48, 66], especially in lower-dimensional cases (i.e., $k = 1, 2$). Its applications to higher-order network analysis remain mostly unexplored. We present a QTSP-based projection algorithm that (approximately) projects a signal \mathbf{s}^k (represented by its simplicial signal state $|\mathbf{s}^k\rangle$) onto its gradient, curl, or harmonic components as described in Eq. (6). Using our QTSP framework given in Theorem 1, we define quantum simplicial filters that approximate the functions Π^G , Π^C which implement projections onto the gradient and the curl spaces (noting that $\Pi^H = \mathbf{I} - \Pi^G - \Pi^C$). Recall the definition of α_k given in the FILTER step, that is, $\alpha_k = \sqrt{n}$ for the direct approach and $\alpha_k = \sqrt{(n+1)(k+1)}$ for the compact approach.

Theorem 2 (QTSP filtering for subcomponent projections). *Let $\xi_{\min}^\ell, \xi_{\min}^u$ be the smallest non-zero singular values of the boundary operators \mathbf{B}_k and \mathbf{B}_{k+1} respectively. Let κ_ℓ, κ_u be such that $1/\kappa_\ell \in (0, \xi_{\min}^\ell/\alpha_k)$, and $1/\kappa_u \in (0, \xi_{\min}^u/\alpha_{k+1})$. Given a simplicial signal state $|\mathbf{s}^k\rangle$ and $\varepsilon_\ell, \varepsilon_u \in (0, 1/2)$, there exist quantum circuits implementing PUEs of quantum simplicial filters $H_{d_\ell+1}^{(\text{SV})}(\mathbf{L}_k^\ell/\alpha_k^2)$ and $H_{d_u+1}^{(\text{SV})}(\mathbf{L}_k^u/\alpha_{k+1}^2)$, with orders $d_\ell + 1 \in O(\kappa_\ell^2 \log((n\kappa_\ell)^2/(\alpha_k^2 \varepsilon_\ell)))$ and $d_u + 1 \in O(\kappa_u^2 \log((n\kappa_u)^2/(\alpha_{k+1}^2 \varepsilon_u)))$ respectively, such that*

$$\begin{aligned} \left\| \Pi^G - 2\kappa_\ell^2 H_{d_\ell+1}^{(\text{SV})}(\mathbf{L}_k^\ell/\alpha_k^2) \right\| &\leq \varepsilon_\ell, \text{ and} \\ \left\| \Pi^C - 2\kappa_u^2 H_{d_u+1}^{(\text{SV})}(\mathbf{L}_k^u/\alpha_{k+1}^2) \right\| &\leq \varepsilon_u. \end{aligned}$$

These circuits have complexity

- (a) (**Direct approach**) $O(dn \log n)$ time and $O(n)$ space,
- (b) (**Compact approach**) $O(dkn^2 \log(n) \log(\log(n)))$ time and $O(k \log n)$ space,

where $d \in \{d_\ell, d_u\}$.

The proof of this theorem is given in Sec. IV D, and naturally follows from Theorem 1 by choosing the appropriate filter $H_d^{(\text{SV})}$.

The subcomponent extraction problem is important in applications such as preference ranking. For example, given pairwise preference data between n elements, one well-studied algorithm for obtaining a global ranking of all elements is HodgeRank [67]. This global ranking is obtained by considering the pairwise preference data as an edge signal \mathbf{s}^1 and projecting onto the gradient component \mathbf{s}_G^1 , which corresponds to a pairwise ranking that is ‘‘globally consistent’’ with the desired total ranking. Theorem 2 states that a filter to perform this projection can be implemented efficiently (polynomially in n, k, d)

on a quantum computer for arbitrary dimension k under certain conditions. This gives a potential application of QTSP filtering beyond what is commonly explored in TSP. We give the details of the application of our algorithm to this problem in Section IV D.

In comparison to Theorem 1, the complexity of implementing the filters described in Theorem 2 has an extra dependence on the smallest singular value of the appropriate boundary operator (which is the square root of the smallest eigenvalue of the corresponding lower or upper Laplacian). This is because the order of the filter required to achieve an accuracy of ε depends on the ratio between the smallest and largest eigenvalues of the corresponding Laplacian. Thus, we note that the complexity is only polynomial in n and k if the spectral gap of the Laplacian is bounded from below by some polynomial in n and k .

While Theorem 1 does not itself require any assumptions about the spectral gap of \mathbf{L}_k , certain applications, such as that given in Theorem 2 (or more generally any application requiring a pseudoinverse) will require a non-vanishing spectral gap. This is somewhat more relaxed than the assumptions required for QTDA, which always requires such a spectral gap, but it is a concern depending on the precise application. In general, the spectral gap of the Hodge Laplacian (and consequently its lower and upper constituents) can be exponentially small in k [68], and so the applicability of Theorem 2 must be analysed on a case-by-case basis depending on the underlying simplicial complex.

It is also worth noting that most of our algorithm described by Theorem 1 does not rely on \mathcal{K} being a clique complex. The restriction to clique complexes is only required so that we can explicitly construct polynomial-depth ‘‘membership functions’’ \mathbf{P}_k that have the action

$$\mathbf{P}_k |\sigma_k\rangle |0\rangle |0\rangle^{\otimes a_p} = |\sigma_k\rangle |\mathbb{1}\{\sigma_k \in \mathcal{K}\}\rangle |0\rangle^{\otimes a_p}, \quad (13)$$

where $\mathbb{1}\{\sigma_k \in \mathcal{K}\} = 1$ if and only if $\sigma_k \in \mathcal{K}$ and is 0 otherwise, $|\sigma_k\rangle$ is a basis state representing a possible k -simplex (some subset of the vertex set \mathcal{V}), and a_p is the number of ancilla qubits used. We do not know how to efficiently implement such a membership oracle for a general simplicial complex. Since these membership functions are implemented $O(d)$ times to create a polynomial of degree d , an efficient implementation of this subroutine is vital to an efficient filtering algorithm. In the case of a clique complex, efficient constructions for membership functions are known. In the case of direct encoding, we employ the circuit given by Berry et al. [39]. We then adapt this to provide an analogous circuit that works for the compact encoding scheme; the exact construction is given in Appendix E.

In the next section, we give the details of the algorithm and prove the complexities given in Theorems 1 and 2. First, we define the simplicial signal state $|\mathbf{s}^k\rangle$ and the direct and compact encodings and review the projected unitary encoding of the boundary operator given by McArdle, Gilyén, and Berta [37]. We focus on the

filter construction for the compact encoding scheme; the results necessary to prove the claims about the direct encoding scheme are given in Appendix D.

IV. DETAILS OF THE QUANTUM ALGORITHM

In this section, we give a detailed description of how to implement the FILTER step, as described in Section III, on a quantum computer for a general polynomial filter. At the end of this section, we show how to apply this framework to the problem of subcomponent extraction. The tools and techniques we use to build our algorithms exist in the literature, and we adapt them to suit our purpose. The main tools are the projected unitary encoding of the boundary operator [35, 37, 39], quantum singular value transformation [44], and linear combinations of unitaries [69].

A. Simplicial signal representation

The first step is to implement an ENCODE subroutine to encode the simplicial signals $\mathbf{s}^k \in \mathbb{R}^{n_k}$ as a quantum state $|\mathbf{s}^k\rangle$, which we formally define below. Broadly speaking, there are two approaches for encoding simplex information in the QTDA literature: a “direct” encoding and a “compact” encoding. In this work, we slightly generalize these encodings to also encode the signals \mathbf{s}^k , rather than just the structure of the simplicial complex. This allows us to encode the signal information using no extra qubits, at the cost of making the signal state more difficult to prepare in general.

The encoding schemes we consider here represent simplices as basis elements and signals as their corresponding amplitudes. To this end, we first define the k -simplicial state $|\sigma_k^i\rangle$, which is a (non-specific) basis encoding for the i -th k -simplex σ_k^i . A simplicial signal can be represented as a collection of pairs $\{(s_i^k, \sigma_k^i)\}_{i \in [n_k]}$, where s_i^k is the signal value on the simplex σ_k^i . Given a basis state $|\sigma_k^i\rangle$ to represent each $\sigma_k^i \in \mathcal{K}$, the k -simplicial signal state $|\mathbf{s}^k\rangle$ is defined as

$$|\mathbf{s}^k\rangle := \frac{1}{\|\mathbf{s}^k\|_2} \sum_{i=0}^{n_k-1} s_i^k |\sigma_k^i\rangle, \quad (14)$$

where $\|\mathbf{s}^k\|_2^2 := \sum_{i=0}^{n_k-1} (s_i^k)^2$ and n_k is the number of k -simplices in the simplicial complex \mathcal{K} . Here $|\mathbf{s}^k\rangle$ is a superposition of all k -simplicial states with amplitudes representing the (normalised) signal values $\{s_i^k\}$. Note that this definition is quite general, as $|\sigma_k^i\rangle$ is as-of-yet undefined.

As previously mentioned, there are two common approaches to representing a k -simplex σ_k as a corresponding (k -)simplicial state $|\sigma_k\rangle$. These are known as the *direct* and *compact* encodings and are given respectively in

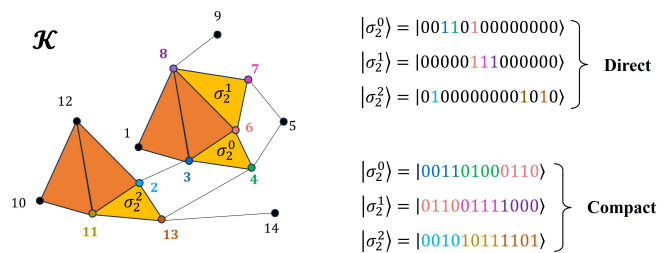


Figure 3. An illustrative example of the direct and compact encodings for three different 2-simplices (3-cliques) in the simplicial complex \mathcal{K} , which is given on the left.

Refs. [39] and [37]. These encodings refer specifically to the qubit representations of simplices $\{\sigma_k^i\}$, which is the pertinent information to QTDA. However, the inclusion of amplitudes $\{s_i^k\}$ is unique to QTSP; in QTDA, these amplitudes are always uniform. The choice of basis encoding affects the construction of the whole algorithm, as it informs the construction of the quantum implementations of the boundary operators. Here we briefly describe both of these basis encodings. An illustrative example of these two encodings for a small complex is given in Figure 3. Recall that the vertex set (equivalently the 0-simplices) of a complex \mathcal{K} are denoted $\{v_1, \dots, v_n\}$.

a. Direct approach. The direct encoding was first proposed in Ref. [32] and is defined as follows on an n -qubit register. A k -simplicial state $|\sigma_k\rangle$ corresponding to a simplex $\sigma_k = \{v_{i_0}, \dots, v_{i_k}\}$ is an n -qubit basis state such that

$$|\sigma_k\rangle := \bigotimes_{i=1}^n |u_i\rangle, \quad \text{where } u_i = \begin{cases} 1, & \text{if } v_i \in \sigma_k, \\ 0, & \text{otherwise.} \end{cases} \quad (15)$$

b. Compact approach. Alternatively, Ref. [37] proposed a representation that uses exponentially fewer qubits when $k = O(\text{polylog}(n))$, and is hence referred to as compact encoding. Let $j \in [k+1] = \{0, \dots, k\}$ and $q_j \in \{1, \dots, n\}$. A k -simplicial state $|\sigma_k\rangle$ is a $((k+1)\lceil \log_2(n+1) \rceil)$ -qubit register such that for any k -simplex $\sigma_k = \{v_{q_j}\}_{j \in [k+1]}$

$$|\sigma_k\rangle := \bigotimes_{j=0}^k |q_j\rangle, \quad (16)$$

for $0 < q_0 < \dots < q_k \leq n$. We call each $|q_j\rangle$ a vertex state. If the filtering task is such that $d_u > 0$ (i.e. the polynomial of the upper Laplacian is not a constant) then there will be an additional register in state $|0\rangle^{\otimes \lceil \log_2(n+1) \rceil}$ to accommodate the additional vertex state that is created by the action of the coboundary operator \mathbf{B}_k^\dagger .

B. Boundary operator construction

In this section we provide a description of the projected unitary encoding (PUE) of the boundary operator

\mathbf{B}_k that we use in the compact encoding scheme, originally given by McArdle, Gilyén, and Berta [37] to study QTDA. This is the main ingredient we use for constructing our quantum simplicial filters. We briefly overview their construction and refer the interested reader to their paper for the full details ([37], Appendix C2). We slightly modify their construction by changing the implementation of the “membership functions” that determine whether an arbitrary basis state represents a simplex in the simplicial complex. We give the specific implemen-

tation in Appendix E. Our membership function is an adaptation of the function given in Refs. [39, 70], which was originally designed for the direct encoding scheme. For the unfamiliar, we also briefly introduce the concept of PUEs defined by Gilyén, Su, Low, and Wiebe [44] in Appendix A, along with a summary of the quantum singular value transformation framework.

Recall that $\alpha_k = \sqrt{(n+1)(k+1)}$ and define $a_k = \lceil \log_2(k+1) \rceil$. Then an $(\alpha_k, a_k, 0)$ -PUE of \mathbf{B}_k is given by Ref. [37] such that

$$\left(\langle 0 |^{\otimes \log_2(k+1)} \otimes \mathbf{I}^s \right) \left(\Pi'_{k-1} \mathbf{U}_{\mathbf{B}_k} \Pi_k \right) \left(|0\rangle^{\otimes \log_2(k+1)} \otimes \mathbf{I}^s \right) = \frac{\mathbf{B}_k}{\alpha_k} =: \mathcal{B}_k, \quad (17)$$

where

$$\begin{aligned} \Pi_k &:= \sum_{\sigma_k \in \mathcal{K}} |\sigma_k\rangle \langle \sigma_k| \\ \Pi'_k &:= \sum_{\sigma_k \in \mathcal{K}} |\sigma_k\rangle \langle \sigma_k| \otimes |0\rangle \langle 0|^{\otimes \log_2(n+1)}, \end{aligned}$$

where the summation range $\sigma_k \in \mathcal{K}$ denotes a summation over all k -simplices in the complex. For neatness, we omit the ceiling functions in the exponents where it is unambiguous. The unitary $\mathbf{U}_{\mathbf{B}_k}$ acts on $(k+1)\lceil \log_2(n+1) \rceil$ qubits, specifically the qubits corresponding to the registers $|q_0\rangle |q_1\rangle \dots |q_k\rangle$ in Eq. (16), as well as an ancilla register of size $\lceil \log_2(k+1) \rceil$. Equivalently, $\mathbf{U}_{\mathbf{B}_{k+1}}$ acts on $(k+2)\lceil \log_2(n+1) \rceil$ and $\lceil \log_2(k+2) \rceil$ qubit registers, where the extra $\lceil \log_2(n+1) \rceil$ -qubit register begins in state $|0\rangle$ and is used when applying the upper Laplacian.

We give a high-level overview of the implementation of $\mathbf{U}_{\mathbf{B}_k}$ given in Ref. [37]. The general idea is to perform a SELECT operation using a $(1/\sqrt{k+1}) \sum_{j=0}^k |j\rangle$ ancilla register that

- (1) swaps the desired vertex state, e.g., $|q_j\rangle$, to the last register of the system qubit registers using controlled-SWAP and integer comparator circuits,
- (2) checks the value of each vertex state register against the values of the adjacent vertex pair registers,
- (3) uncomputes the $(1/\sqrt{k+1}) \sum_{j=0}^k |j\rangle$ ancilla qubit, and
- (4) implements Hadamard gates to the last register.

The result of this unitary applied to some state $|q_0\rangle |q_1\rangle \dots |q_k\rangle$ is to create a superposition of states $|q_0\rangle |q_1\rangle \dots |q_j\rangle \dots |q_{k-1}\rangle |x\rangle$ for each $j \in [k+1]$ and all $x \in [n+1]$, where $|q_j\rangle$ denotes that this register is not present. Then, the projector Π'_{k-1} zeroes out any basis state where $x \neq 0$. The operator $\mathbf{U}_{\mathbf{B}_k}$ has a non-Clifford gate depth of $O(k \log(\log(n)))$ and requires $O(\log(k))$ ancilla qubits.

To complete the description of this PUE, we need to give an implementation of the C_{Π_k} NOT gate, which has the action

$$C_{\Pi_k} \text{NOT} := \Pi_k \otimes \mathbf{X} + (\mathbf{I} - \Pi_k) \otimes \mathbf{I}, \quad (18)$$

as well as an implementation of the $C_{\Pi'_k}$ NOT gate. The analogous function given in Ref. [37] does not quite suit our purpose, as it was designed with persistent homology in mind. Recall from Eq. (13) that \mathbf{P}_k is the so-called membership function defined by the action

$$\mathbf{P}_k |\sigma_k\rangle |a\rangle |0\rangle^{\otimes a_p} = |\sigma_k\rangle |a \oplus \mathbb{1}\{\sigma_k \in \mathcal{K}\}\rangle |0\rangle^{\otimes a_p},$$

where $a \in \{0, 1\}$, a_p is the number of ancilla qubits, and $\mathbb{1}\{\sigma_k \in \mathcal{K}\}$ is the indicator function for the event that $\sigma_k \in \mathcal{K}$ for some $\sigma_k \subseteq \mathcal{V}$. Constructions for C_{Π_k} NOT and $C_{\Pi'_k}$ NOT follow immediately from a construction for \mathbf{P}_k . In Appendix E, we give an explicit construction for \mathbf{P}_k when the simplicial states are described by the compact encoding scheme. This circuit has a non-Clifford gate depth of $O(n^2 k \log(n))$ and uses $O(k)$ ancillas. Additionally, note that the procedure and cost of implementing the PUEs of the adjoint operators \mathbf{B}_k^\dagger and \mathbf{B}_{k+1}^\dagger follow from the fact that $\mathbf{U}_{\mathbf{A}^\dagger} = \mathbf{U}_{\mathbf{A}}^\dagger$.

C. Filter construction

A simplicial filter $H(\mathbf{L}_k^\ell, \mathbf{L}_k^u)$ is comprised of polynomials of \mathbf{L}_k^ℓ and \mathbf{L}_k^u , as given in Eq. (7). As described in the FILTER step in Section III, we implement simplicial filters of the form

$$\begin{aligned} H_d^{(\text{SV})}(\mathcal{L}_k^\ell, \mathcal{L}_k^u) &:= \sum_{i_\ell=0}^{d_\ell} \mathfrak{h}_{i_\ell}^\ell(\mathcal{B}_k)^{2i_\ell} \\ &\quad + \sum_{i_u=0}^{d_u} \mathfrak{h}_{i_u}^u(\mathcal{B}_{k+1})^{2i_u} - \mathfrak{h}_0 \mathbf{I}, \quad (19) \end{aligned}$$

where $\mathcal{B}_k = \mathbf{B}_k/\alpha_k$ is defined in Eq. (17) for the compact encoding, $\mathcal{L}_k^\ell := \mathcal{B}_k^\dagger \mathcal{B}_k$, and $\mathcal{L}_k^u := \mathcal{B}_{k+1}^\dagger \mathcal{B}_{k+1}$. This is inspired by the Chebyshev filter design in Eq. (11) but with

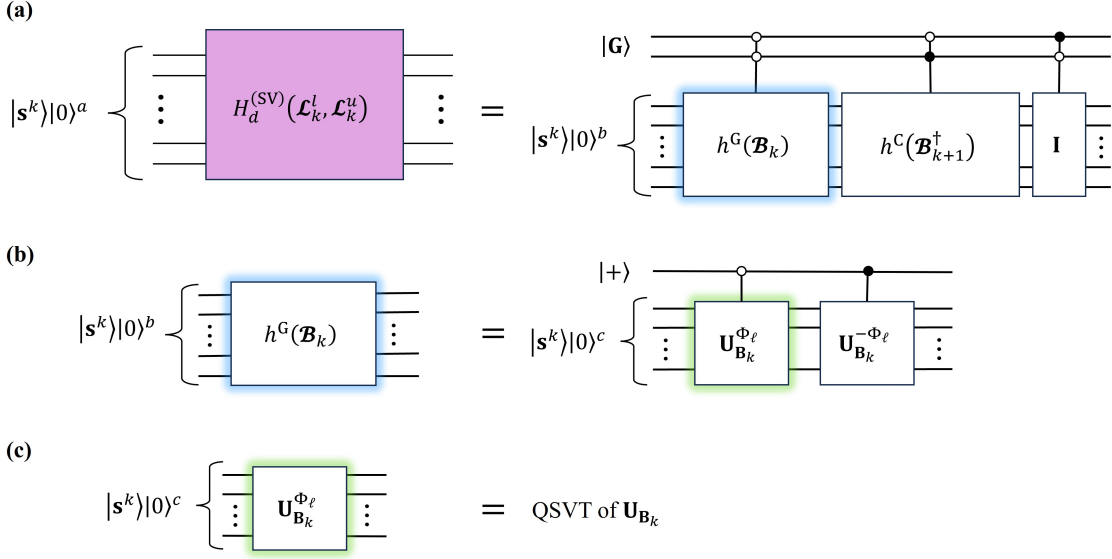


Figure 4. (a) A quantum simplicial filter $H_d^{(SV)}(\mathcal{L}_k^\ell, \mathcal{L}_k^u)$ is a linear combination of two polynomials $h^G(\mathcal{B}_k)$, $h^C(\mathcal{B}_{k+1}^\dagger)$, and an identity operator \mathbf{I} . (b) A PUE of a real-valued polynomial $h^G(\mathcal{B}_k)$. (c) A polynomial transformation of \mathcal{B}_k by QSVT.

a different rescaling factor so that it is more amenable to implementation on a quantum computer. This multi-variable polynomial of \mathcal{L}_k^ℓ and \mathcal{L}_k^u can be constructed by implementing the *linear combination of unitaries* (LCU) method [69] and the *quantum singular value transformation* (QSVT) [44], which is a versatile quantum algorithm used to construct polynomial transformations of any matrix in a quantum circuit. For completeness, we briefly review the LCU method and QSVT algorithm in Appendices A and B.

The combination of the LCU method and QSVT enables us to construct different degree and parity polynomials of different matrices in a single call to a quantum operation called the *SELECT* operation (we refer readers to Appendix A for the definition of the *SELECT* operation). To this end, we give a slight generalization of Lemma 52 in Ref. [44] combined with the construction of general polynomials given in Ref. [71], which produces a projected unitary encoding of a linear combination of complex-valued polynomials. Here, we define a set of matrices $\{\mathbf{A}_i\}_{i \in [m]}$, all with the same dimensions, acting on the same Hilbert space.

Lemma 1 (PUE of a Linear Combination of Complex-Valued Polynomials). *Let $\{f_i(x)\}_{i \in [m]}$ be a set of complex-valued polynomials such that $\Re(f_i(x)) = g_{\mathbb{R},i}(x)$ and $\Im(f_i(x)) = h_{\mathbb{S},i}(x)$ are real-valued polynomials of degree $d_{\mathbb{R},i}$ and $d_{\mathbb{S},i}$ with definite parities. Suppose that $|g_{\mathbb{R},i}(x)| \leq 1$ and $|h_{\mathbb{S},i}(x)| \leq 1$ for all $x \in [-1, 1]$ and $i \in [m]$. Let $\mathbf{U}_{\mathbf{A}_i}$ be a $(1, a_i, 0)$ -PUE of \mathbf{A}_i for each $i \in [m]$. Then there exist sequences of phase factors $\{\Phi_{g_i}, \Phi_{h_i}\}_{i \in [m]}$ implementing a $(\beta, a + \lceil \log(2m) \rceil + 3, 0)$ -PUE of $\sum_{i=0}^{m-1} c_i f_i(\mathbf{A}_i)$, where*

$$c_i \in \mathbb{R}_+, \beta := \|c\|_1, \text{ and } a := \left(\sum_{i=0}^{m-1} a_i \right).$$

Moreover, let $\delta \in \mathbb{R}_+$ be arbitrary and define $d = \max(d_{\mathbb{R},0}, \dots, d_{\mathbb{R},m-1}, d_{\mathbb{S},0}, \dots, d_{\mathbb{S},m-1})$. Then using $O(\text{poly}(d, \log(1/\delta)))$ classical computation time, sequences of phase factors $\{\Phi'_{g_i}, \Phi'_{h_i}\}_{i \in [m]}$ can be found which implement a $(\beta, a + \lceil \log(2m) \rceil + 3, \beta\delta)$ -PUE of $\sum_{i=0}^{m-1} c_i f_i(\mathbf{A}_i)$.

The proof is given in Appendix F. For our purposes, we employ this lemma to construct a PUE of $H^{(SV)}(\mathcal{L}_k^\ell, \mathcal{L}_k^u)$ from PUEs of \mathcal{B}_k and \mathcal{B}_k^\dagger (defined in Eq. (17) for the compact encoding). The basic outline of this design is as follows: assume that the frequency responses g^G, g^C are (or are approximated by) degree- d polynomials on $[0, 1]$ such that $g^G(0) = g^C(0) = \mathfrak{h}_0$ and $|g^G(x)| \leq 1, |g^C(x)| \leq 1$. We suppose that g^G and g^C are given by $\sum_{i=0}^{d_i} \mathfrak{h}_{i_i}^\ell x^{i_i}$ and $\sum_{i_u=0}^{d_u} \mathfrak{h}_{i_u}^u x^{i_u}$ respectively. Then, given the coefficients of these polynomials, a PUE of the filter given in Eq. (19) is constructed by combining Lemma 1 with the PUEs of \mathcal{B}_k and \mathcal{B}_k^\dagger . The construction of a quantum simplicial filter is given in the following lemma. Recall that INPUT_c , as defined in Section III, is the set of classical inputs given to the quantum computer, consisting of the signal \mathbf{s}^k as a vector as well as the filter coefficients $\{\mathfrak{h}_0, \mathfrak{h}_{i_\ell}^\ell, \mathfrak{h}_{i_u}^u\}$. Recall that a_p is the number of ancilla qubits used in the operator \mathbf{P}_k .

Lemma 2 (PUE of quantum simplicial filter). *Given INPUT_c , there exists a quantum circuit implementing a $(\beta, a_k + a_{k+1} + a_p + 6, 0)$ -PUE of the quantum simplicial filter $H_d^{(SV)}(\mathcal{L}_k^\ell, \mathcal{L}_k^u)$, where $\beta := 2 + \mathfrak{h}_0$ and a_p is the ancilla cost in the membership function. This quantum cir-*

circuit uses $4d_\ell$ calls each to $\mathbf{U}_{\mathbf{B}_k}$ and $\mathbf{U}_{\mathbf{B}_k}^\dagger$, $4d_u$ calls each to $\mathbf{U}_{\mathbf{B}_{k+1}}$ and $\mathbf{U}_{\mathbf{B}_{k+1}}^\dagger$, $8d_\ell$ calls each to $\mathbf{C}_{\Pi_{k-1}} \text{NOT}$ and $\mathbf{C}_{\Pi_k} \text{NOT}$, $8d_u$ calls each to $\mathbf{C}_{\Pi_k} \text{NOT}$ and $\mathbf{C}_{\Pi_{k+1}} \text{NOT}$, and $O(\max\{d_\ell, d_u\})$ calls to single qubit rotation gates.

The complexity cost of PUE of the quantum simplicial filter, and thus the proof of Theorem 1, follows immediately from Lemma 2 and is given below (with the direct encoding details given in Appendix D).

Proof of Theorem 1. We assume we are given the simplicial state $|\mathbf{s}^k\rangle$ from the ENCODE step. Given filter coefficients $\{\mathfrak{h}_0, \mathfrak{h}_{i_\ell}^\ell, \mathfrak{h}_{i_u}^u\}$ for $i_\ell \in [d_\ell + 1]$ and $i_u \in [d_u + 1]$ as part of INPUT_c , Lemma 2 states that there exists a quantum circuit that implements a PUE of $H_d^{(\text{SV})}(\mathcal{L}_k^\ell, \mathcal{L}_k^u)$. This lemma also describes the complexity and ancilla costs in terms of d_ℓ, d_u , and the costs of implementing $\mathbf{U}_{\mathbf{B}_k}$, $\mathbf{U}_{\mathbf{B}_{k+1}}$, and $\mathbf{C}_{\Pi_k} \text{NOT}$. The FILTER step as described in Section III simply consists of applying the quantum simplicial filter, i.e. the PUE of $H_d^{(\text{SV})}(\mathcal{L}_k^\ell, \mathcal{L}_k^u)$, to the state $|\mathbf{s}^k\rangle$. Thus, the complexity cost of implementing the FILTER step is given as follows:

a. Direct approach. The unitary operators $\mathbf{U}_{\mathbf{B}_k}$ and $\mathbf{U}_{\mathbf{B}_{k+1}}$ each have non-Clifford gate depth $O(\log n)$. Each $\mathbf{C}_{\Pi_k} \text{NOT}$ or $\mathbf{C}_{\Pi_{k+1}} \text{NOT}$ requires one call to a z -rotation and two calls to the k -simplex-identifying function \mathbf{P}_k , which gives a non-Clifford gate depth $O(n \log n)$ [37, 72]. Therefore, the total non-Clifford gate depth of the quantum simplicial filter is $O(dn \log n)$, where $d = \max(d_\ell, d_u)$. The number of ancilla qubits used in this circuit is $O(n)$, dominated by the application of \mathbf{P}_k .

b. Compact approach. In this approach, both the operators $\mathbf{U}_{\mathbf{B}_k}$ and $\mathbf{U}_{\mathbf{B}_{k+1}}$ have non-Clifford gate depth $O(k \log \log(n))$. Each $\mathbf{C}_{\Pi_k} \text{NOT}$ or $\mathbf{C}_{\Pi_{k+1}} \text{NOT}$ requires one call to a z -rotation and two calls to the k -simplex-identifying function \mathbf{P}_k . The implementation of \mathbf{P}_k given in Appendix E has non-Clifford gate depth $O(n^2 k \log n)$. Therefore, the total non-Clifford depth of the quantum simplicial filter is $O(dkn^2 \log n \log \log n)$. Lastly, the number of ancilla qubits used in this circuit is $O(k)$, again dominated by implementing the simplex-identifying circuit. \square

D. QTSP filtering for Hodge decomposition

Here we prove Theorem 2 about signal subcomponent extraction based on the Hodge decomposition. Given a signal $\mathbf{s}^k \in \mathbb{R}^{n_k}$, the Hodge decomposition states that $\mathbf{s}^k = \mathbf{s}_H^k + \mathbf{s}_G^k + \mathbf{s}_C^k$, where $\mathbf{s}_H^k \in \ker(\mathbf{L}_k)$, $\mathbf{s}_G^k \in \text{im}(\mathbf{B}_k^\dagger)$, and $\mathbf{s}_C^k \in \text{im}(\mathbf{B}_{k+1})$. We design quantum simplicial filters that approximately extract each of these (normalized) components. We do this by employing Theorem 1 and applying a filter that approximates a projection onto each of the subspaces defined by the Hodge decomposition. We do this by modifying a construction for the Moore-Penrose pseudoinverse of a projected unitary encoding,

in our case of the upper or lower Laplacians respectively. Constructions for implementing the Moore-Penrose pseudoinverse via QSVT are given by Refs. [36, 44].

We first define some notation to discuss the construction of the pseudoinverse of a matrix \mathbf{A} , which is denoted by \mathbf{A}^+ . Let $\{\lambda_i\}_{i \in [m]}$ be the eigenvalues of a Hermitian matrix \mathbf{A} . Then $\xi_i = \sqrt{\lambda_i}$, for $i \in [m]$, are the singular values of $\sqrt{\mathbf{A}}$ (where $\sqrt{\mathbf{A}}$ is the matrix such that $\mathbf{A} = \sqrt{\mathbf{A}}^\dagger \mathbf{A}$). The condition number of \mathbf{A} is given by $\kappa(\mathbf{A}) = \|\mathbf{A}\|_2 \|\mathbf{A}^{-1}\|_2 = \lambda_{\max}/\lambda_{\min}$, while the effective condition number of $\sqrt{\mathbf{A}}$ is given by $\kappa_{\text{eff}}(\sqrt{\mathbf{A}}) = \kappa_{\text{eff}}(\sqrt{\mathbf{A}^\dagger}) = \sqrt{\kappa(\mathbf{A})} = \xi_{\max}/\xi_{\min}$.

The main idea of extracting subcomponents based on the Hodge decomposition is to project \mathbf{s}^k to the gradient and curl subspaces, $\text{im}(\mathbf{B}_k^\dagger)$ and $\text{im}(\mathbf{B}_{k+1})$. Mathematically speaking, this is done by implementing projection operators Π^G and Π^C with the action $\Pi^G \mathbf{s}^k = \mathbf{s}_G^k$ and $\Pi^C \mathbf{s}^k = \mathbf{s}_C^k$. It has been shown [4, 48, 67] that these projectors are equivalent to

$$\begin{aligned} \Pi^G &= \mathbf{B}_k^\dagger (\mathbf{L}_{k-1}^u)^+ \mathbf{B}_k, \text{ and} \\ \Pi^C &= \mathbf{B}_{k+1} (\mathbf{L}_{k+1}^\ell)^+ \mathbf{B}_{k+1}^\dagger, \end{aligned} \quad (20)$$

where $\mathbf{L}_{k-1}^u = \mathbf{B}_k \mathbf{B}_k^\dagger$ and $\mathbf{L}_{k+1}^\ell = \mathbf{B}_{k+1}^\dagger \mathbf{B}_{k+1}$. This can be seen by recalling that $\mathbf{B}_k \mathbf{B}_{k+1} = \mathbf{0}$ for all $k \geq 0$ and the fact that the pseudoinverse finds the (Euclidean) norm-minimising solution. We note here again that we can also construct the projector onto the harmonic space by $\Pi^H = \mathbf{I} - \Pi^G - \Pi^C$.

One way to implement the Moore-Penrose pseudoinverse of a matrix via QSVT is to implement a polynomial $f : [-1, 1] \rightarrow [-1, 1]$ which closely approximates $1/x$ on a domain that contains the singular values of the matrix in question. Such a polynomial was given by Gilyén, Su, Low, and Wiebe [44] (Theorem 41), which is a modification of a polynomial given by Childs, Kothari, and Somma [69]. To construct the projection operators given in Eq. (20), we modify this polynomial slightly and then apply it to the PUE of the boundary operator using QSVT. Notably, if g_d is the degree- d polynomial approximation to $1/x$, then we implement the polynomial $H_{d+1} : [-1, 1] \rightarrow [-1, 1]$ defined by $H_{d+1}(x) = x^2 g_d(x^2)$. It follows (shown in detail in Appendix H) that for sufficiently large d ,

$$H_{d+1}^{(\text{SV})}(\mathbf{L}_k^\ell) = \mathbf{B}_k^\dagger g_d(\mathbf{L}_{k-1}^u) \mathbf{B}_k \approx \Pi^G. \quad (21)$$

Similarly, for sufficiently large d it follows that $H_{d+1}^{(\text{SV})}(\mathbf{L}_k^u) \approx \Pi^C$. Consequently, the projection operators are also simply polynomials of \mathbf{B}_k and \mathbf{B}_{k+1}^\dagger : if g_d is a degree- d polynomial, then H_{d+1} is a degree- $(2d+2)$ polynomial of \mathbf{B}_k or \mathbf{B}_{k+1}^\dagger (equivalently, a degree- $(d+1)$ polynomial of \mathbf{L}_k^ℓ or \mathbf{L}_k^u). In our QTSP filtering framework, we can construct such a polynomial using Lemma 2 and calculate the construction costs using Theorem 1. Define $\kappa_\ell := \kappa_{\text{eff}}(\mathbf{B}_k)$ and $\kappa_u := \kappa_{\text{eff}}(\mathbf{B}_{k+1})$. To account

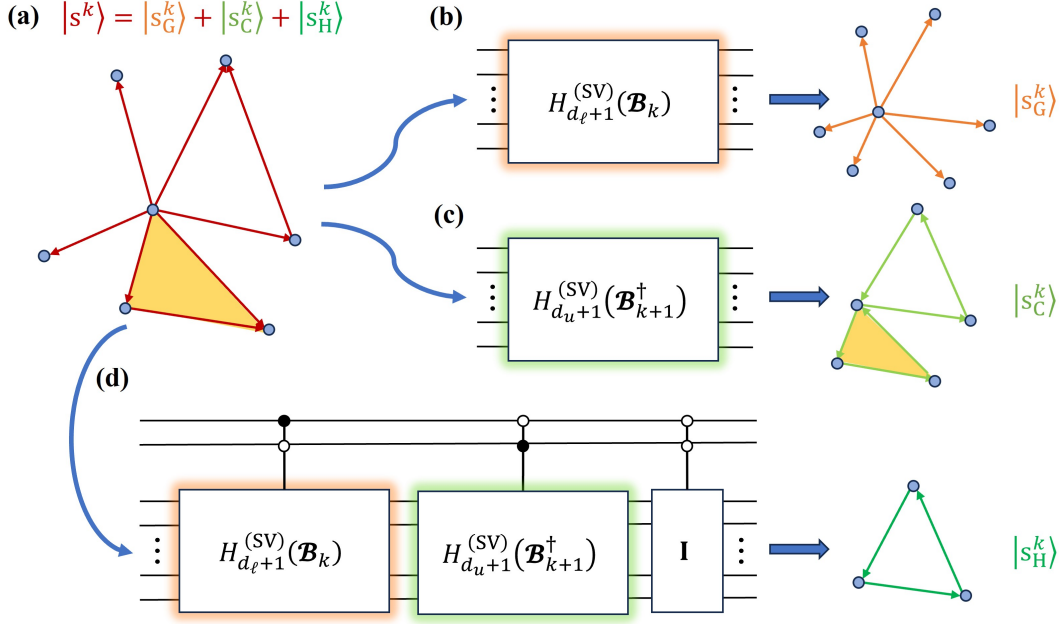


Figure 5. QTSP filtering for subcomponents extraction. (a) The input simplicial signal state $|\mathbf{s}^k\rangle$ decomposed into three orthogonal signal states based on Hodge decomposition. (b) A quantum simplicial filter projecting $|\mathbf{s}^k\rangle$ into the gradient part $|\mathbf{s}_G^k\rangle$. (c) A quantum simplicial filter projecting $|\mathbf{s}^k\rangle$ into the curl part $|\mathbf{s}_C^k\rangle$. (d) A quantum simplicial filter combining gradient and curl projectors employed to project $|\mathbf{s}^k\rangle$ into the harmonic part $|\mathbf{s}_H^k\rangle$.

for the approximation error and the rescaling inherent in the PUE of the projector, we state the existence of polynomials approximating the gradient and curl projections in the QTSP filtering framework as follows.

Lemma 3 (Polynomial Approximation of Subcomponent Projection). *Let Π^G, Π^C be projection operators to the $\text{im}(\mathcal{B}_k^\dagger)$ and $\text{im}(\mathcal{B}_{k+1})$ subspaces respectively. Then given $\varepsilon_\ell, \varepsilon_u \in (0, \frac{1}{2})$, there exist $d_\ell \in O(\kappa_\ell^2 \log((n\kappa_\ell)^2/(\alpha_{\bar{k}}^2 \varepsilon_\ell)))$ and $d_u \in O(\kappa_u^2 \log((n\kappa_u)^2/(\alpha_{\bar{k}+1}^2 \varepsilon_u)))$ such that there exist degree- $2d_\ell+2$ and $2d_u+2$ polynomials of \mathcal{B}_k and $\mathcal{B}_{k+1}^\dagger$, denoted by $H_{d_\ell+1}^{(SV)}(\mathcal{L}_k^\ell)$ and $H_{d_u+1}^{(SV)}(\mathcal{L}_k^u)$, satisfying*

$$\begin{aligned} \left\| \Pi^G - 2\kappa_\ell^2 H_{d_\ell+1}^{(SV)}(\mathcal{L}_k^\ell) \right\| &\leq \varepsilon_\ell, \text{ and} \\ \left\| \Pi^C - 2\kappa_u^2 H_{d_u+1}^{(SV)}(\mathcal{L}_k^u) \right\| &\leq \varepsilon_u. \end{aligned}$$

The proof of the lemma is given in Appendix H. The proof is an application and straightforward modification of the results by Hayakawa [36] and Gilyén, Su, Low, and Wiebe [44] about using QSVT to implement the Moore-Penrose pseudoinverse. Theorem 2 then follows by combining Lemma 3 and Theorem 1 to calculate the cost of implementing the simplicial filter described in the lemma using our framework. The proof of Theorem 2 is given below.

Proof of Theorem 2. Given the polynomial coefficients of $H_{d_\ell+1}^{(SV)}(\mathcal{L}_k^\ell)$ and $H_{d_u+1}^{(SV)}(\mathcal{L}_k^u)$ from Lemma 3 (given in

Appendix H), Lemma 2 guarantees that there exist sequences of phase factors $\Phi_G \in \mathbb{R}^{2d_\ell+2}$ and $\Phi_C \in \mathbb{R}^{2d_u+2}$, and the corresponding phased alternating sequences $\mathbf{U}_{\mathcal{B}_k}^{\Phi_G}$ and $\mathbf{U}_{\mathcal{B}_{k+1}^\dagger}^{\Phi_C}$ that construct a $(2\kappa_\ell^2, a_\ell + 1, \varepsilon_\ell)$ -PUE of Π^G and a $(2\kappa_u^2, a_u + 1, \varepsilon_u)$ -PUE of Π^C . Then the complexity of each quantum simplicial filter follows from Theorem 1 and the bounds on d_ℓ and d_u given in Lemma 3. \square

It is worth noting that in certain applications of the Hodge decomposition (for example, statistical ranking [67]) recovery of the projected vector is not the last step in the process. In the case of statistical ranking, the desired vector is actually a vector \mathbf{s}^{k-1} such that $\mathbf{B}_k^T \mathbf{s}^{k-1} = \mathbf{s}_G^k$, whose existence is guaranteed by the Hodge decomposition. By implementing slightly different polynomials (specifically $H'_{d+1}(x) = xg_d(x^2)$ instead of $H_{d+1}(x) = x^2g_d(x^2)$, see Remark 2 in Appendix H for details), we can implement a PUE of an operator that outputs \mathbf{s}^{k-1} instead of \mathbf{s}_G^k . This allows one to skip the step of solving for \mathbf{s}^{k-1} using \mathcal{B}_k and \mathbf{s}_G^k , which could be expensive when n_k , the number of k -simplices, is very large.

V. DISCUSSION

This work presents a quantum algorithm implementing TSP filtering processes in higher-order networks modelled by simplicial complexes using QSVT and tools from QTDA. The type of filter we implement, described in

Eq. (12) is inspired by the Chebyshev filter design given in [51]. When the number of simplicial signals scales exponentially in the number of vertices, our algorithm runs linearly in the dimension k of the simplices considered. In comparison, the worst-case complexity of the best-known algorithm for general classical TSP filtering tasks is exponential in the dimension.

Nevertheless, we do not make any rigorous claims of a quantum speedup, as this potential advantage comes with some caveats that must be first accounted for. Firstly, a filtering task must be chosen so that the encoding and retrieving of the simplicial signals encoded in quantum states can be done efficiently. This includes post-selecting on the ancilla register being in the correct state, which is a complexity that is not accounted for in this work. Secondly, we also require that the task is, in some rough sense, insensitive to the scaling factor of $\|\mathbf{s}^k\|^{-1}$ in the signals and the factors of α_k and α_{k+1} introduced in the filter.

A natural future direction for research would be a rigorous comparison between the classical and quantum algorithms, accounting for the aforementioned caveats in full to determine the nature of any advantage. Approximate filtering algorithms do not seem to be well studied in the classical literature, but would be a more apt comparison point than the exact algorithms given in Refs. [50, 51] that we have used as a reference point. For example, Black and Nayyeri [73] gave a method for solving the equation $\mathbf{L}_1 \mathbf{x} = \mathbf{b}$ which runs nearly linearly in n and polynomially in β_1 , the first Betti number. A deeper exploration of classical approximation algorithms could be combined with looking at other methods for building quantum simplicial filters, such as multivariable QSP as described by Rossi and Chuang [74], in order to determine the optimal way to build quantum simplicial filters.

Another future direction would be to find quantum sensor data with the form of a simplicial signal state and

to use the QTSP framework for analysing this data. Such an application would sidestep the difficulties inherent in the ENCODE step. In terms of more general applications, TSP on classical computers has been mostly studied for low dimensional cases, i.e. $k \leq 2$. As such, a broader avenue for future research would be to explore the possible applications of TSP to higher-order networks when $k > 2$. This is a large, open-ended question of independent interest, but it would also help inform the aforementioned analysis of the possibility of a practical speedup using the QSVT framework for classical data.

Finally, one application of classical TSP that has recently received some attention is in the area of neural networks, where simplicial filters are used to construct simplicial neural networks, which are generalisations of graph neural networks [52]. The idea is to add a nonlinear function w to alter the filtering process such that the input-output relationship is

$$\mathbf{s}_{\text{out}}^k = w \left(H(\mathbf{L}_k^\ell, \mathbf{L}_k^u) \mathbf{s}_{\text{in}}^k \right), \quad (22)$$

where $\mathbf{s}_{\text{in}}^k, \mathbf{s}_{\text{out}}^k$ are the input and output simplicial signals. Then one optimizes the filter coefficients to approximate the desired output simplicial signal. It is suggested that this nonlinearity introduced in the neural network approach allows for more expressive modelling of higher-order interactions [52, 75, 76]. It would be interesting to see if simplicial neural networks could be implemented more efficiently on fault-tolerant quantum computers via QSVT algorithms [77, 78].

ACKNOWLEDGEMENTS

We thank Yuval R. Sanders for several technical discussions. C.M.G.L is supported by a Monash Graduate Scholarship.

-
- [1] A. Sandryhaila and J. M. F. Moura. Discrete signal processing on graphs. *IEEE Transactions on Signal Processing*, 61(7):1644–1656, 2013.
 - [2] A. Sandryhaila and J. M. F. Moura. Discrete signal processing on graphs: Frequency analysis. *IEEE Transactions on Signal Processing*, 62(12):3042–3054, 2014.
 - [3] A. Ortega, P. Frossard, J. Kovacevic, J. M. F. Moura, and P. Vandergheynst. Graph Signal Processing: Overview, Challenges, and Applications. *Proceedings of the IEEE*, 106(5):808–828, 2018.
 - [4] S. Barbarossa and S. Sardellitti. Topological Signal Processing over Simplicial Complexes. *IEEE Transactions on Signal Processing*, 68:2992–3007, 2020.
 - [5] M. T. Schaub, Y. Zhu, J. B. Seby, T. M. Roddenberry, and S. Segarra. Signal processing on higher-order networks: Livin’ on the edge. and beyond. *Signal Processing*, 187, 2021.
 - [6] F. Battiston, G. Cencetti, I. Iacopini, V. Latora, M. Lucas, A. Patania, J-G. Young, and G. Petri. Networks beyond pairwise interactions: Structure and dynamics. *Physics Reports*, 874:1–92, 2020.
 - [7] F. Battiston, E. Amico, A. Barrat, G. Bianconi, G. F. de Arruda, B. Franceschiello, I. Iacopini, S. Kéfi, V. Latora, Y. Moreno, M. M. Murray, T. P. Peixoto, F. Vaccarino, and G. Petri. The physics of higher-order interactions in complex systems. *Nature Physics*, 17(10):1093–1098, 2021.
 - [8] S. Majhi, M. Perc, and D. Ghosh. Dynamics on higher-order networks: A review. *Journal of the Royal Society Interface*, 19(188), 2022.
 - [9] C. Bick, E. Gross, H. A. Harrington, and M. T. Schaub. What Are Higher-Order Networks? *SIAM Review*, 65(3):686–731, 2023.
 - [10] L. Calmon, M. T. Schaub, and G. Bianconi. Dirac signal processing of higher-order topological signals, 2023.

- arXiv:2301.10137.
- [11] I. Jablonski. Graph Signal Processing in Applications to Sensor Networks, Smart Grids, and Smart Cities. *IEEE Sensors Journal*, 17(23):7659–7666, 2017.
 - [12] W. Huang, L. Goldsberry, N. F. Wymbs, S. T. Grafton, D. S. Bassett, and A. Ribeiro. Graph Frequency Analysis of Brain Signals. *IEEE Journal on Selected Topics in Signal Processing*, 10(7):1189–1203, 2016.
 - [13] L. Goldsberry, W. Huang, N. F. Wymbs, S. T. Grafton, D. S. Bassett, and A. Ribeiro. Brain Signal Analytics from Graph Signal Processing Perspective. *IEEE Signal Processing Society*, page 851, 2017.
 - [14] W. Huang, T. A. W. Bolton, J. D. Medaglia, D. S. Bassett, A. Ribeiro, and D. Van De Ville. A graph signal processing perspective on functional brain imaging. *Proceedings of the IEEE*, 106(5):868–885, 2018.
 - [15] S. Segarra, A. G. Marques, G. Mateos, and A. Ribeiro. Network topology inference from spectral templates. *IEEE Transactions on Signal and Information Processing over Networks*, 3(3):467–483, 2017.
 - [16] V. K. Sharma, D. K. Srivastava, and P. Mathur. Efficient image steganography using graph signal processing. *IET Image Processing*, 12(6):1065–1071, 2018.
 - [17] G. Cheung, E. Magli, Y. Tanaka, and M. K. Ng. Graph Spectral Image Processing, 2018.
 - [18] M. Lucas, G. Cencetti, and F. Battiston. Multiorder Laplacian for synchronization in higher-order networks. *Physical Review Research*, 2(3), 2020.
 - [19] A. Patania, G. Petri, and F. Vaccarino. The shape of collaborations. *EPJ Data Science*, 6(1), 2017.
 - [20] Z. Cang, L. Mu, K. Wu, K. Opron, K. Xia, and G-W. Wei. A topological approach for protein classification. *Computational and Mathematical Biophysics*, 3(1), 2015.
 - [21] Gunnar Carlsson. Topology and Data. *Bulletin of the American Mathematical Society*, 46(2):255–308, 2009.
 - [22] A. Patania, F. Vaccarino, and G. Petri. Topological analysis of data. *EPJ Data Science*, 6(1), 2017.
 - [23] L. Wasserman. Topological Data Analysis. *Annual Review of Statistics and Its Applications*, 5:501–532, 2018.
 - [24] F. Chazal and B. Michel. An Introduction to Topological Data Analysis: Fundamental and Practical Aspects for Data Scientists. *Frontiers in Artificial Intelligence*, 4, 2021.
 - [25] V. de Silva and R. Ghrist. Coverage in sensor networks via persistent homology. *Algebraic and Geometric Topology*, 7(1):339–358, 2007.
 - [26] M. Gidea and Y. Katz. Topological data analysis of financial time series: Landscapes of crashes. *Physica A: Statistical Mechanics and its Applications*, 491:820–834, 2018.
 - [27] T. Qaiser, Y. W. Tsang, D. Taniyama, N. Sakamoto, K. Nakane, D. Epstein, and N. Rajpoot. Fast and accurate tumor segmentation of histology images using persistent homology and deep convolutional features. *Medical Image Analysis*, 55:1–14, 2019.
 - [28] C. J. Carstens and K. J. Horadam. Persistent homology of collaboration networks. *Mathematical Problems in Engineering*, 2013, 2013.
 - [29] H. Adams, T. Emerson, M. Kirby, R. Neville, C. Peterson, P. Shipman, S. Chepushtanova, E. Hanson, F. Motta, and L. Ziegelmeier. Persistence Images: A Stable Vector Representation of Persistent Homology. *Journal of Machine Learning Research*, 18:1–35, 2017.
 - [30] A. J. Blumberg, I. Gal, M. A. Mandell, and M. Pancia. Robust Statistics, Hypothesis Testing, and Confidence Intervals for Persistent Homology on Metric Measure Spaces. *Foundations of Computational Mathematics*, 14(4):745–789, 2014.
 - [31] F. Hensel, M. Moor, and B. Rieck. A survey of topological machine learning methods. *Frontiers in Artificial Intelligence*, 4, 2021.
 - [32] S. Lloyd, S. Garnerone, and P. Zanardi. Quantum algorithms for topological and geometric analysis of data. *Nature Communications*, 7, 2016.
 - [33] C. Cade and P. M. Crichigno. Complexity of supersymmetric systems and the cohomology problem, 2021. arXiv:2107.00011.
 - [34] C. Gyurik, C. Cade, and V. Dunjko. Towards Quantum Advantage via Topological Data Analysis. *Quantum*, 6:1–31, 2022.
 - [35] I. Y. Akhalwaya, S. Ubaru, K. L. Clarkson, M. S. Squillante, V. Jejjala, Y-H. He, K. Naidoo, V. Kalantzis, and L. Horesh. Towards quantum advantage on noisy quantum computers, 2022. arXiv:2209.09371.
 - [36] R. Hayakawa. Quantum algorithm for persistent Betti numbers and topological data analysis. *Quantum*, 6, 2022.
 - [37] S. McArdle, A. Gilyén, and M. Berta. A Streamlined Quantum Algorithm for Topological Data Analysis with Exponentially Fewer Qubits, 2022. arXiv:2209.12887.
 - [38] A. Schmidhuber and S. Lloyd. Complexity-Theoretic Limitations on Quantum Algorithms for Topological Data Analysis, 2022. arXiv:2209.14286.
 - [39] D. W. Berry, Y. Su, C. Gyurik, R. King, J. Basso, A. Del Toro Barba, A. Rajput, N. Wiebe, V. Dunjko, and R. Babbush. Analyzing prospects for quantum advantage in topological data analysis, 2023. arXiv:2209.13581.
 - [40] Y. R. Sanders, D. W. Berry, P. C.S. Costa, L. W. Tessler, N. Wiebe, C. Gidney, H. Neven, and R. Babbush. Compilation of fault-tolerant quantum heuristics for combinatorial optimization. *PRX Quantum*, 1:020312, 2020.
 - [41] R. Babbush, J. R. McClean, M. Newman, C. Gidney, S. Boixo, and H. Neven. Focus beyond Quadratic Speedups for Error-Corrected Quantum Advantage. *PRX Quantum*, 2(1), 2021.
 - [42] G. H. Low and I. L. Chuang. Optimal Hamiltonian Simulation by Quantum Signal Processing. *Physical Review Letters*, 118(1), 2017.
 - [43] G. H. Low and I. L. Chuang. Hamiltonian simulation by qubitization. *Quantum*, 3, 2019.
 - [44] A. Gilyén, Y. Su, G. H. Low, and N. Wiebe. Quantum singular value transformation and beyond: Exponential improvements for quantum matrix arithmetics. In *Proceedings of the Annual ACM Symposium on Theory of Computing*, pages 193–204. Association for Computing Machinery, 2019.
 - [45] L. Lin and Y. Tong. Optimal polynomial based quantum eigenstate filtering with application to solving quantum linear systems. *Quantum*, 4, 2020.
 - [46] L. Lin and Y. Tong. Near-optimal ground state preparation. *Quantum*, 4, 2020.
 - [47] P. C. S. Costa, D. An, Y. R. Sanders, Y. Su, R. Babbush, and D. W. Berry. Optimal scaling quantum linear-systems solver via discrete adiabatic theorem. *PRX Quantum*, 3:040303, 2022.
 - [48] L. H. Lim. Hodge Laplacians on Graphs. *SIAM Review*, 62(3):685–715, 2020.

- [49] Timothy E Goldberg. Combinatorial laplacians of simplicial complexes. Senior Thesis, Bard College, 6, 2002.
- [50] M. Yang, E. Isufi, M. T. Schaub, and G. Leus. Finite Impulse Response Filters for Simplicial Complexes. In European Signal Processing Conference, volume 2021-August, pages 2005–2009. European Signal Processing Conference, EUSIPCO, 2021.
- [51] M. Yang, M. T. Isufi, E. and Schaub, and G. Leus. Simplicial Convolutional Filters. IEEE Transactions on Signal Processing, 2021-August:4633–4648, 2022.
- [52] S. Ebli, M. Defferrard, and G. Spreemann. Simplicial neural networks, 2020. arXiv:2010.03633.
- [53] D. I. Shuman, P. Vandergheynst, and P. Frossard. Chebyshev polynomial approximation for distributed signal processing. In 2011 International Conference on Distributed Computing in Sensor Systems and Workshops (DCOSS), pages 1–8, 2011.
- [54] F. Baccini, F. Geraci, and G. Bianconi. Weighted simplicial complexes and their representation power of higher-order network data and topology. Physical Review E, 106(3), 2022.
- [55] S. Krishnagopal and G. Bianconi. Spectral detection of simplicial communities via Hodge Laplacians. Physical Review E, 104(6), 2021.
- [56] A. W. Harrow, A. Hassidim, and S. Lloyd. Quantum algorithm for linear systems of equations. Physical Review Letters, 103(15), 2009.
- [57] P. Reberntrost, M. Mohseni, and S. Lloyd. Quantum support vector machine for big data classification. Physical Review Letters, 113(3), 2014.
- [58] S. Lloyd, M. Mohseni, and P. Reberntrost. Quantum principal component analysis. Nature Physics, 10(9):631–633, 2014.
- [59] I. Kerenidis and A. Prakash. Quantum recommendation system. In Leibniz International Proceedings in Informatics, LIPIcs, volume 67. Schloss Dagstuhl-Leibniz-Zentrum fur Informatik GmbH, Dagstuhl Publishing, 2017.
- [60] I. Kerenidis, J. Landman, A. Luongo, and A. Prakash. Q-means: A quantum algorithm for unsupervised machine learning. In Proceedings of the 33rd International Conference on Neural Information Processing Systems, 2019.
- [61] I. Kerenidis and J. Landman. Quantum spectral clustering. Physical Review A, 103(4), 2021.
- [62] S. Aaronson. Read the fine print. Nature Physics, 11(4):291–293, 2015.
- [63] X. M. Zhang, T. Li, and X. Yuan. Quantum State Preparation with Optimal Circuit Depth: Implementations and Applications. Physical Review Letters, 129(23), 2022.
- [64] J. van Apeldoorn, A. Cornelissen, A. Gilyén, and G. Nannicini. Quantum tomography using state-preparation unitaries. In Proceedings of the 2023 Annual ACM-SIAM Symposium on Discrete Algorithms (SODA), pages 1265–1318, 2023.
- [65] J. Friedman. Computing Betti Numbers via Combinatorial Laplacians. Algorithmica, 21, 1998.
- [66] H. Bhatia, G. Norgard, V. Pascucci, and P. T. Bremer. The Helmholtz-Hodge decomposition - A survey. IEEE Transactions on Visualization and Computer Graphics, 19(8):1386–1404, 2013.
- [67] X. Jiang, L. H. Lim, Y. Yao, and Y. Ye. Statistical ranking and combinatorial Hodge theory. Mathematical Programming, 127(1):203–244, 2011.
- [68] J. Steenbergen, C. Klivans, and S. Mukherjee. A cheeger-type inequality on simplicial complexes. Advances in Applied Mathematics, 56:56–77, 2014.
- [69] A. M. Childs, R. Kothari, and R. D. Somma. Quantum algorithm for systems of linear equations with exponentially improved dependence on precision. SIAM Journal on Computing, 46(6):1920–1950, 2017.
- [70] S. A. Metwalli, F. Le Gall, and R. Van Meter. Finding Small and Large k -Clique Instances on a Quantum Computer. IEEE Transactions on Quantum Engineering, 1:1–11, 2021.
- [71] Y. Dong, X. Meng, K. B. Whaley, and L. Lin. Efficient phase-factor evaluation in quantum signal processing. Physical Review A, 103(4), 2021.
- [72] I. Kerenidis and A. Prakash. Quantum machine learning with subspace states, 2022. arXiv:2202.00054.
- [73] M. Black and A. Nayyeri. Hodge Decomposition and General Laplacian Solvers for Embedded Simplicial Complexes. In Leibniz International Proceedings in Informatics, LIPIcs, volume 229. Schloss Dagstuhl-Leibniz-Zentrum fur Informatik GmbH, Dagstuhl Publishing, 2022.
- [74] Z. M. Rossi and I. L. Chuang. Multivariable quantum signal processing (M-QSP): prophecies of the two-headed oracle. Quantum, 6, 2022.
- [75] T. M. I. Roddenberry, N. Glaze, and S. Segarra. Principled simplicial neural networks for trajectory prediction. In M. Meila and T. Zhang, editors, Proceedings of the 38th International Conference on Machine Learning, volume 139 of Proceedings of Machine Learning Research, pages 9020–9029. PMLR, 18–24 Jul 2021.
- [76] A. D. Keros, V. Nanda, and K. Subr. Dist2Cycle: A Simplicial Neural Network for Homology Localization. In 36th AAAI Conference on Artificial Intelligence, 2022.
- [77] N. Guo, K. Mitarai, and K. Fujii. Nonlinear transformation of complex amplitudes via quantum singular value transformation, 2021. arXiv:2107.10764.
- [78] Arthur G. R. and P. Reberntrost. Non-linear transformations of quantum amplitudes: Exponential improvement, generalization, and applications, 2023. arXiv:2309.09839.
- [79] D. W. Berry, A.M. Childs, and R. Kothari. Hamiltonian Simulation with Nearly Optimal Dependence on all Parameters. In Proceedings - Annual IEEE Symposium on Foundations of Computer Science, FOCS, volume 2015-December, pages 792–809. IEEE Computer Society, 2015.
- [80] D. W. Berry, A. M. Childs, R. Cleve, R. Kothari, and R. D. Somma. Simulating hamiltonian dynamics with a truncated taylor series. Physical Review Letters, 114(9), 2015.
- [81] J. M. Martyn, Z. M. Rossi, A. K. Tan, and I. L. Chuang. Grand Unification of Quantum Algorithms. PRX Quantum, 2(4), 2021.
- [82] I. Y. Akhalwaya, Y-H. He, L. Horesh, W. Jejjala, V. and Kirby, K. Naidoo, and S. Ubaru. Representation of the fermionic boundary operator. Physical Review A, 106(2), 2022.
- [83] S. A. Cuccaro., T. G. Draper, S. A. Kutin., and D. P. Moulton. A new quantum ripple-carry addition circuit, 2004. arXiv:quant-ph/0410184.
- [84] D. Horak and J. Jost. Spectra of combinatorial Laplace operators on simplicial complexes. Advances in Mathematics, 244, 2013.

Appendix A: Projected unitary encodings of arbitrary matrices

Here we describe general methods from the literature that are used to implement non-unitary operators in quantum circuits. We give a brief overview of the linear combination of unitaries, block encodings, and projected unitary encodings for unfamiliar readers, as we use these to build quantum circuits that implement polynomials of the upper and lower Laplacians \mathbf{L}_k^ℓ and \mathbf{L}_k^u . This is a brief summary of ideas from Refs. [44, 79–81], and we refer interested readers to these papers for more details.

If the desired operator is Hermitian, a common approach to implementing it in a quantum circuit is to do a Hamiltonian simulation [56], where a Hermitian matrix \mathbf{H} is encoded in a unitary matrix $\mathbf{U}_\mathbf{H} = e^{i\mathbf{H}t}$. The linear combination of unitaries (LCU) method [79, 80] is one of the avenues for implementing Hamiltonian simulation which has had wide applicability in implementing many different operators in quantum circuits. In this paper, we use this to combine polynomials of the lower and upper Hodge Laplacians to create our desired quantum simplicial filter.

The description of the LCU technique, as given in Refs. [79, 80] is as follows. Let $\mathbf{A} = \sum_{i=0}^{m-1} c_i \mathbf{A}_i$ be a linear combination of a set of unitaries \mathbf{A}_i with a set of coefficients $c_i \in \mathbb{R}_+$. Let $(\mathbf{G} \otimes \mathbf{I}^s)$ be a so-called PREPARE operation such that

$$\mathbf{G}|0\rangle^{\otimes \log_2 n} = \frac{1}{\sqrt{\|c\|_1}} \sum_{i=1}^n \sqrt{c_i} |i\rangle := |\mathbf{G}\rangle, \quad (\text{A1})$$

where $\|c\|_1 := \sum_{i=1}^n |c_i|$. The SELECT operation is then defined as

$$\mathbf{W} := \sum_{i=1}^n |i\rangle\langle i| \otimes \mathbf{A}_i. \quad (\text{A2})$$

Then the transformation $|\psi\rangle \mapsto \frac{\mathbf{A}|\psi\rangle}{\|\mathbf{A}|\psi\rangle\|}$ can be done by applying $\text{PREPARE}^\dagger \cdot \text{SELECT} \cdot \text{PREPARE}$ to $|0\rangle^{\otimes \log_2 n} \otimes |\psi\rangle$ and post-selecting the ancilla qubit register on the state $|00\dots 0\rangle$. The success probability of post-selection is $\frac{\|\mathbf{A}|\psi\rangle\|^2}{\|c\|_1^2}$.

An improvement of the LCU technique in terms of precision and complexity is given by the block-encoding (BE) technique. This technique was first developed within the framework of qubitization [43], which directly encodes a Hermitian matrix \mathbf{H} into the unitary operator $\mathbf{U}_\mathbf{H}$ as

$$\mathbf{U}_\mathbf{H} = \begin{bmatrix} \mathbf{H}/\alpha & * \\ * & * \end{bmatrix},$$

where the $*$ denotes a block of the matrix $\mathbf{U}_\mathbf{H}$ with arbitrary entries that ensure that $\mathbf{U}_\mathbf{H}$ is unitary. We follow the presentation of block-encoding given in Ref. [44].

Definition 1 (Block-Encoding (BE)). *Suppose \mathbf{H} is a Hermitian matrix. A (α, a, ε) -block encoding of a Hermitian matrix \mathbf{H} is a unitary matrix $\mathbf{U}_\mathbf{H}$ such that*

$$\left\| \mathbf{H} - \alpha \left(|0\rangle^{\otimes a} \otimes \mathbf{I}^s \right) \mathbf{U}_\mathbf{H} \left(|0\rangle^{\otimes a} \otimes \mathbf{I}^s \right) \right\| \leq \varepsilon, \quad (\text{A3})$$

where $\alpha \in \mathbb{R}_+$ is the scaling factor, $a \in \mathbb{N}$ is the number of ancilla qubits, and $\varepsilon \in \mathbb{R}_+$ is an arbitrary small number representing the error (in operator norm).

As is done in the above definition, the notation \mathbf{I}^x is used to denote the identity operator acting on ancilla qubit register which has x qubits, and \mathbf{I}^s is the identity operator acting on the system qubit register.

The idea of a block encoding of a Hermitian matrix can be generalised to any arbitrary matrix \mathbf{A} using what is called a projected unitary encoding of \mathbf{A} . Let $\mathbf{A} \in \mathbb{C}^{m' \times m}$ be a $(m' \times m)$ -matrix with complex entries. Then the *singular value decomposition* (SVD) of \mathbf{A} is given by $\mathbf{A} = \mathbf{V}_L \mathbf{\Sigma} \mathbf{V}_R^\dagger$, where $\mathbf{\Sigma} \in \mathbb{R}^{m' \times m}$ is a diagonal matrix with entries $\Sigma_{ii} := \xi_i \geq 0$ for all $i \in [\min\{m', m\}]$, which are called the *singular values* of \mathbf{A} , and $\{\mathbf{V}_L \in \mathbb{C}^{m' \times m'}, \mathbf{V}_R \in \mathbb{C}^{m \times m}\}$ are a pair of unitary matrices in which each column of \mathbf{V}_L is called a left singular vector $|v_l\rangle$ and each row of \mathbf{V}_R is called a right singular vector $\langle v_r|$.

Definition 2 (Projected Unitary Encoding (PUE)). *Suppose $\mathbf{A} \in \mathbb{C}^{m_l \times m_r}$ and the SVD of \mathbf{A} is written as $\mathbf{A} := \sum_{i=1}^{\min\{m_l, m_r\}} \xi_i |v_l^i\rangle\langle v_r^i|$. Let $\Pi' := \sum_{i=1}^{m_l} |v_l^i\rangle\langle v_l^i|$ and $\Pi := \sum_{i=1}^{m_r} |v_r^i\rangle\langle v_r^i|$ be orthogonal projectors projecting all vectors*

into the space spanned by the left and right singular vectors respectively. A (α, a, ε) -projected unitary encoding of matrix \mathbf{A} is a unitary matrix

$$\mathbf{U}_{\mathbf{A}} = \Pi' \begin{bmatrix} \mathbf{A}/\alpha & * \\ * & * \end{bmatrix},$$

where Π, Π' locate \mathbf{A} within $\mathbf{U}_{\mathbf{A}}$ such that

$$\left\| \mathbf{A} - \alpha \left(|0\rangle^{\otimes a} \otimes \mathbf{I}^s \right) \left(\Pi' \mathbf{U}_{\mathbf{A}} \Pi \right) \left(|0\rangle^{\otimes a} \otimes \mathbf{I}^s \right) \right\| \leq \varepsilon,$$

where $\alpha \in \mathbb{R}_+$ is the scaling factor, $a \in \mathbb{N}$ is the number of ancilla qubits being used, and $\varepsilon \in \mathbb{R}_+ \cup \{0\}$ is an arbitrary small number representing the error.

Within this framework, a (α, a, ε) -BE of \mathbf{H} can be seen as a (α, a, ε) -PUE of \mathbf{H} with $\Pi' = \Pi = |0\rangle\langle 0|^{\otimes a} \otimes \mathbf{I}^s$.

Appendix B: Quantum algorithm for constructing polynomials (QSVT)

In this section we give a brief background to the quantum singular value transformation, as well as a statement of the result itself. This paper uses the notations defined in Ref. [44]. Let $\mathbb{C}[x]$ be the space of all complex-valued polynomial functions such that for $f \in \mathbb{C}[x]$, $f(x) = \sum_{i=0}^{d-1} c_i x^i$ and $f^*(x) = \sum_{i=0}^{d-1} c_i^* x^i$, where $c_i \in \mathbb{C}$ for all $i \in [d]$ and $*$ is the complex conjugation operation. Additionally, the real and imaginary parts of f are denoted as $\Re(f)(x) = \sum_{i=0}^{d-1} \Re(c_i) x^i$ and $\Im(f)(x) = \sum_{i=0}^{d-1} \Im(c_i) x^i$, respectively. If $\mathbf{A} = \sum_{i=1}^{\min\{m', m\}} \xi_i |v_l^i\rangle\langle v_r^i|$ is the SVD of a matrix \mathbf{A} , then given $f \in \mathbb{C}[x]$, a degree- d polynomial transformation of a matrix \mathbf{A} is described as $f(\mathbf{A}) = \sum_{i=0}^{\min\{m', m\}-1} f(\xi_i) |v_r^i\rangle\langle v_r^i|$ when d is even and $f(\mathbf{A}) = \sum_{i=0}^{\min\{m', m\}-1} f(\xi_i) |v_l^i\rangle\langle v_l^i|$ when d is odd.

The idea of polynomial transformation originated from the *quantum signal processing* (QSP) theorem [42, 43], which builds a matrix consisting of special complex-valued polynomials using a sequence of reflection operators.

Theorem 3 (Quantum Signal Processing (QSP) by Reflection, Corollary 8 [44]). *Let $\mathbf{R}(x)$ be a parametrized family of single qubit reflections, where*

$$\mathbf{R}(x) := \begin{bmatrix} x & \sqrt{1-x^2} \\ \sqrt{1-x^2} & -x \end{bmatrix}$$

for all $x \in [-1, 1]$. There exists a sequence of phase factors $\Phi := (\phi_1, \dots, \phi_d) \in \mathbb{R}^d$ such that

$$\begin{aligned} \mathbf{U}_x^\Phi &:= \prod_{i=1}^d \left(e^{i\phi_i \mathbf{Z}} \mathbf{R}(x) \right) \\ &= \begin{bmatrix} P(x) & * \\ * & * \end{bmatrix}, \end{aligned}$$

where $P \in \mathbb{C}^d[x]$ satisfies the following properties:

- C1. The parity of $P(x)$ is $d \bmod 2$;
- C2. $|P(x)| \leq 1$, for all $x \in [-1, 1]$, whereas $|P(x)| \geq 1$ otherwise;
- C3. If d is even, $P(ix)P^*(ix) \geq 1$, for all $x \in \mathbb{R}$.

The relation between the QSP theorem and Jordan's lemma, stating that the product of two reflection operators is a rotation, can be found in Ref. [44]. Many standard quantum computing subroutines such as amplitude amplification can be seen as a polynomial transformation of x [81].

The quantum singular value transformation is a generalization of *quantum eigenvalue transformation* (QET) [43, 81], which combines QSP with *qubitization* to implement polynomials of Hermitian matrices.

Theorem 4 (Quantum Eigenvalue Transformation, Theorem 3 [81]). *Let $\mathbf{U}_{\mathbf{H}}$ be a (α, a, ε) -block encoding of a Hermitian matrix \mathbf{H} as defined in Definition 1. Let $\text{Poly}(x)$ be a degree- d polynomial satisfying C1–C3 in Theorem 3. Then there exists a sequence of phase factors $\Phi := (\phi_1, \dots, \phi_d) \in \mathbb{R}^d$ such that*

$$\text{Poly}(\mathbf{H}/\alpha) = \left(\langle 0 |^{\otimes a} \otimes \mathbf{I} \right) \left(\Pi \mathbf{U}_{\mathbf{H}}^{\Phi} \Pi \right) \left(|0\rangle^{\otimes a} \otimes \mathbf{I} \right) \quad (\text{B1})$$

where $\Pi := |0\rangle\langle 0|^{\otimes a} \otimes \mathbf{I}$, and

$$\mathbf{U}_{\mathbf{H}}^{\Phi} := \begin{cases} \prod_{i=1}^{d/2} \left(e^{i\phi_{2i-1}(2\Pi-\mathbf{I})} \mathbf{U}_{\mathbf{H}}^{\dagger} e^{i\phi_{2i}(2\Pi-\mathbf{I})} \mathbf{U}_{\mathbf{H}} \right), & \text{for } d \text{ even,} \\ e^{i\phi_1(2\Pi-\mathbf{I})} \mathbf{U}_{\mathbf{H}} \prod_{i=1}^{(d-1)/2} \left(e^{i\phi_{2i}(2\Pi-\mathbf{I})} \mathbf{U}_{\mathbf{H}}^{\dagger} e^{i\phi_{2i+1}(2\Pi-\mathbf{I})} \mathbf{U}_{\mathbf{H}} \right), & \text{for } d \text{ odd.} \end{cases}$$

The matrix representation of $\mathbf{U}_{\mathbf{H}}^{\Phi}$ is described by

$$\mathbf{U}_{\mathbf{H}}^{\Phi} = \begin{bmatrix} \text{Poly}(H/\alpha) & * \\ * & * \end{bmatrix}, \quad (\text{B2})$$

where again the $*$ denotes a block of the matrix $\mathbf{U}_{\mathbf{H}}^{\Phi}$ with arbitrary entries that ensure that $\mathbf{U}_{\mathbf{H}}^{\Phi}$ is unitary.

While the QET algorithm only implements a polynomial transformation of Hermitian matrices, the quantum singular value transformation [44] constructs a polynomial transformation for any matrix. We state the QSVT theorem based on the presentation in Ref. [81].

Theorem 5 (Quantum Singular Value Transformation (QSVT), Theorem 4 [81]). *Let $\mathbf{U}_{\mathbf{A}}$ be a (α, a, ε) -PUE (as in Definition 2) of a matrix \mathbf{A} . Let $\text{Poly}(x)$ be a degree- d polynomial satisfying C1–C3 in Theorem 3. Then there exists a sequence of phase factors $\Phi := (\phi_1, \dots, \phi_d) \in \mathbb{R}^d$ such that*

$$\text{Poly}^{(\text{SV})}(\mathbf{A}/\alpha) = \begin{cases} \left(\langle 0 |^{\otimes a} \otimes \mathbf{I}^s \right) \left(\Pi \mathbf{U}_{\mathbf{A}}^{\Phi} \Pi \right) \left(|0\rangle^{\otimes a} \otimes \mathbf{I}^s \right), & \text{for } d \text{ even,} \\ \left(\langle 0 |^{\otimes a} \otimes \mathbf{I}^s \right) \left(\Pi' \mathbf{U}_{\mathbf{A}}^{\Phi} \Pi \right) \left(|0\rangle^{\otimes a} \otimes \mathbf{I}^s \right), & \text{for } d \text{ odd,} \end{cases} \quad (\text{B3})$$

where Π' , Π are defined in Definition 2, and the phased alternating sequence $\mathbf{U}_{\mathbf{A}}^{\Phi}$ is given by

$$\mathbf{U}_{\mathbf{A}}^{\Phi} := \begin{cases} \prod_{i=1}^{d/2} \left(e^{i\phi_{2i-1}(2\Pi-\mathbf{I}^s)} \mathbf{U}_{\mathbf{A}}^{\dagger} e^{i\phi_{2i}(2\Pi-\mathbf{I}^s)} \mathbf{U}_{\mathbf{A}} \right), & \text{for } d \text{ even,} \\ e^{i\phi_1(2\Pi'-\mathbf{I}^s)} \mathbf{U}_{\mathbf{A}} \prod_{i=1}^{(d-1)/2} \left(e^{i\phi_{2i}(2\Pi-\mathbf{I}^s)} \mathbf{U}_{\mathbf{A}}^{\dagger} e^{i\phi_{2i+1}(2\Pi'-\mathbf{I}^s)} \mathbf{U}_{\mathbf{A}} \right), & \text{for } d \text{ odd.} \end{cases}$$

Moreover, $\mathbf{U}_{\mathbf{A}}^{\Phi}$ can be implemented by calling to $\mathbf{U}_{\mathbf{A}}$ and $\mathbf{U}_{\mathbf{A}}^{\dagger}$ d times, and $\text{C}_{\Pi'}\text{NOT}$ and C_{Π}NOT $2d$ times, where

$$\text{C}_{\Pi}\text{NOT} := \Pi \otimes \mathbf{X} + (\mathbf{I} - \Pi) \otimes \mathbf{I}.$$

The matrix representation of $\mathbf{U}_{\mathbf{A}}^{\Phi}$ is described by

$$\mathbf{U}_{\mathbf{A}}^{\Phi} = \begin{bmatrix} \text{Poly}^{(\text{SV})}(\mathbf{A}/\alpha) & * \\ * & * \end{bmatrix}. \quad (\text{B4})$$

Although the above method only constructs complex-valued polynomials satisfying conditions C1–C3 in Theorem 3, combining the LCU method and QSVT algorithm allows one to implement a wider range of polynomials, especially real-valued polynomials. Based on the fact that the real part of any complex-valued function is given by $\Re(f(x)) = 1/2(f(x) + f^*(x))$, one can find a real-valued polynomial $\text{Poly}_{f_{\Re}}^{(\text{SV})}(\mathbf{A}) := \Re(\text{Poly}_f^{(\text{SV})}(\mathbf{A}))$ from a linear combination of $\mathbf{U}_{\mathbf{A}}^{\Phi_f}$ and $\mathbf{U}_{\mathbf{A}}^{-\Phi_f}$.

Corollary 1 (QSVT by Real-Valued Polynomials, Corollary 10 and 18 [44]). *Let $f_{\Re} \in \mathbb{R}^d[x]$ be a (either even or odd parity) real-valued polynomial of degree d satisfying $|f_{\Re}(x)| \leq 1$ for all $x \in [-1, 1]$. Let $\mathbf{U}_{\mathbf{A}}, \Pi', \Pi$ be as in Theorem 5. Then there exists $\Phi_f \in \mathbb{R}^d$ such that*

$$f_{\Re}^{(\text{SV})}(\mathbf{A}) = \left(\langle + | \otimes \left(\langle 0 |^{\otimes a} \otimes \mathbf{I}^s \right) \right) \mathbf{W}_{f_{\Re}} \left(|+\rangle \otimes \left(|0\rangle^{\otimes a} \otimes \mathbf{I}^s \right) \right)$$

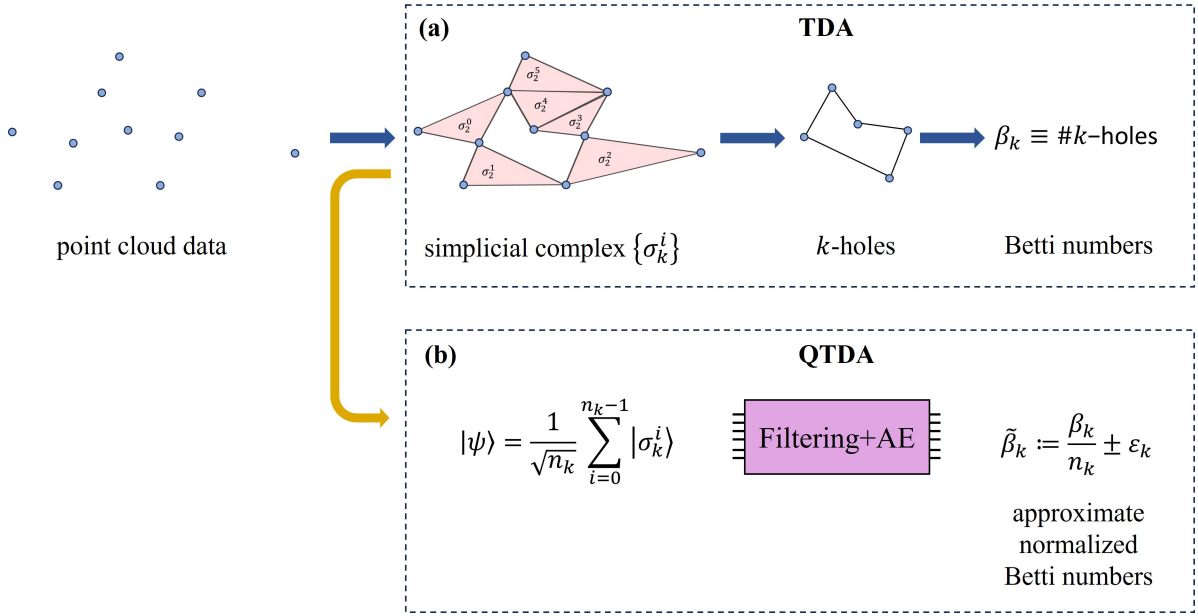


Figure 6. (a) A high-level picture of the TDA pipeline. The left-to-right flow of blue arrows describes taking some point cloud data, constructing a simplicial complex from this data, extracting the kernel of the corresponding Hodge Laplacian, and counting the dimension of the kernel to determine the Betti numbers; (b) a high-level picture of the QTDA pipeline utilizing eigenstate filtering and amplitude estimation (AE) algorithms to determine approximate, normalized Betti numbers.

where

$$\mathbf{W}_{f_{\Re}} := \begin{cases} |0\rangle\langle 0| \otimes \Pi \mathbf{U}_{\mathbf{A}}^{\Phi_f} \Pi + |1\rangle\langle 1| \otimes \Pi \mathbf{U}_{\mathbf{A}}^{-\Phi_f} \Pi, & \text{for } d \text{ is even} \\ |0\rangle\langle 0| \otimes \Pi' \mathbf{U}_{\mathbf{A}}^{\Phi_f} \Pi + |1\rangle\langle 1| \otimes \Pi' \mathbf{U}_{\mathbf{A}}^{-\Phi_f} \Pi, & \text{for } d \text{ is odd.} \end{cases}$$

Moreover, given $f_{\Re} \in \mathbb{R}^d[x]$ and $\delta > 0$, using $O(\text{poly}(d, \log(1/\delta)))$ classical computation time one can find a sequence of phase factors $\Phi'_f \in \mathbb{R}^d$ and a corresponding polynomial $\text{Poly}_{f_{\Re}}^{(\text{SV})}$ such that

$$\left\| f_{\Re}(\mathbf{A}) - \text{Poly}_{f_{\Re}}^{(\text{SV})}(\mathbf{A}) \right\| \leq \delta.$$

Note that one can also find an approximation of a purely imaginary-valued polynomial by observing that $i\Im(f(x)) = 1/2(f(x) - f^*(x))$. Therefore, one can use $W_{i f_{\Im}} := (\mathbf{Z} \otimes \mathbf{I}^{a+s+1}) W_{f_{\Re}}$ to construct $\text{Poly}_{i f_{\Im}}^{(\text{SV})}(\mathbf{A}/\alpha)$.

One important application of this algorithm is implementing the Moore-Penrose pseudoinverse, a generalisation of the inverse matrix to arbitrary matrices. For an arbitrary matrix \mathbf{A} with singular value decomposition $\mathbf{A} = \mathbf{W}\mathbf{\Sigma}\mathbf{V}^\dagger$, the Moore-Penrose pseudoinverse of \mathbf{A} is given by $\mathbf{A}^+ := \mathbf{V}\mathbf{\Sigma}^+\mathbf{W}^\dagger$, where $\mathbf{\Sigma}^+$ is the diagonal matrix obtained by inverting the nonzero entries of $\mathbf{\Sigma}$, which are the singular values of \mathbf{A} , and leaving the zero entries unchanged. QSVT can be used to implement unitaries approximating the pseudoinverse of a matrix \mathbf{A} encoded in some unitary $\mathbf{U}_{\mathbf{A}}$ by approximating $1/x$ with polynomials. Such an approximation is given in Theorem 41 of Ref. [44], as well as Appendix C of Ref. [81]. For $\kappa > 1$, $\varepsilon \in (0, 1/2)$, and $x \in [-1, 1] \setminus [-1/\kappa, 1/\kappa]$, they show that there exists a polynomial $g^+ \in \mathbb{R}^d[x]$ with degree $d \in O(\kappa \log(\kappa/\varepsilon))$ that $\frac{\varepsilon}{2\kappa}$ -approximates $\frac{1}{2\kappa x}$ on the domain $[-1, 1] \setminus [-1/\kappa, 1/\kappa]$. Furthermore, $|g^+(x)| \leq 1$ for all $x \in [-1, 1]$ and $g^+(0) = 0$. Thus, given g^+ with $\kappa := \kappa(\mathbf{A})$, Corollary 1 guarantees that there exists a sequence of phase factors $\Phi_+ \in \mathbb{R}^d$ and $\mathbf{U}_{\mathbf{A}}^{\Phi_+}$ such that $(|0\rangle^{\otimes a} \otimes \mathbf{I}^s) \mathbf{U}_{\mathbf{A}}^{\Phi_+} (|0\rangle^{\otimes a} \otimes \mathbf{I}^s) = g^+(\mathbf{A})$ satisfies $\|\mathbf{A}^+ - 2\kappa g^+(\mathbf{A})\| \leq \varepsilon$.

Appendix C: A brief overview of QTDA

TDA utilizes the topological invariants, extracted from the simplicial structure of point cloud data, as signatures of the dataset. The key subroutine of this method is an algorithm to find the dimension of the kernel of the Hodge Laplacian, known as the Betti number. One begins with mapping the data in a high-dimensional space and constructing a

simplicial complex in such a space. The next step is then constructing the Hodge Laplacian of the simplicial complex and obtaining its kernel. The last step is computing the rank of the kernel. Figure 6(a) shows the high-level picture of this subroutine. In recent QTDA algorithm given by McArdle, Gilyén, and Berta [37], given classical information of the underlying graph, they tackle such a problem by encoding the simplices as an initial quantum state, constructing the corresponding boundary operation in a quantum circuit, projecting the initial quantum state to the kernel of the Hodge Laplacian via a QSVT-based eigenstate filtering, and finding the dimension of the Hodge Laplacian by utilizing a QSVT-based amplitude estimation algorithm. As the quantum algorithms rescale the Betti number, one can only estimate the approximation of the normalized Betti numbers. We depict this pipeline in Figure 6(b).

Appendix D: Projected unitary encoding of the boundary operator for the direct encoding

Here we give a brief summary of the PUE of the boundary operator for basis states represented in the direct encoding, as well as its complexity. This approach is used in some previous QTDA literature [35, 39, 72]. At a high level, the action of the boundary operator in this approach is can be described by a superposition of n tensor products of n Pauli operators, in which each i -th operator flips the qubit in the i -th location in $|\sigma_k\rangle$ and changes the sign based on the number of 1s before the i -th qubit. This operator is called the *fermionic Dirac operator* \mathbf{D} , presented in Ref. [82] and given by

$$\mathbf{D} := \sum_{i=0}^{n-1} \mathbf{Z}^{\otimes(i-1)} \otimes \mathbf{X} \otimes \mathbf{I}^{\otimes(i-1)}. \quad (\text{D1})$$

The action of this operator on a k -simplicial state (basis state corresponding to a k -simplex in the direct encoding, given in (15)) gives a superposition of $(k-1)$ - and $(k+1)$ -simplicial states. However, the output of the boundary operator should only consist of $(k-1)$ -simplices, and not all the resulting states even correspond to simplices in \mathcal{K} . This is because \mathbf{D} outputs all possible $(k+1)$ -simplicial states, which include states that do not necessarily represent co-faces of σ_k . This operator is transformed into a PUE of \mathbf{B}_k by applying the appropriate left and right projectors. Recall the definition of the k -simplex identifying oracle \mathbf{P}_k with the action $\mathbf{P}_k |\sigma_k\rangle |0\rangle = |\sigma_k\rangle |\mathbb{1}\{\sigma_k \in \mathcal{K}\}\rangle$ which checks if a given $|\sigma_k\rangle$ is in the simplicial complex \mathcal{K} (by an abuse of notation, we use the same notation for \mathbf{P}_k as in the compact encoding). An implementation of \mathbf{P}_k for the direct encoding for the case where $\mathcal{K} = \mathcal{K}(G)$ is a clique complex is given in Refs. [39, 70]. Using a Clifford loader circuit given in Ref. [72], we can implement a $(\alpha_k, 0, 0)$ -PUE of \mathbf{B}_k in the direct encoding as

$$\Pi_{k-1} \mathbf{D} \Pi_k = \frac{\mathbf{B}_k}{\alpha_k}, \quad (\text{D2})$$

where $\Pi_{k-1} = \sum_{\sigma_{k-1} \in \mathcal{K}} |\sigma_{k-1}\rangle \langle \sigma_{k-1}|$, $\Pi_k = \sum_{\sigma_k \in \mathcal{K}} |\sigma_k\rangle \langle \sigma_k|$ (where the sums are over all $(k-1)$ - and k -simplices respectively) act as the projection operators defined in Definition 2, and $\alpha_k = \sqrt{n}$ for all k . The implementation of \mathbf{D} requires a non-Clifford gate depth of $O(\log(n))$ and zero ancilla qubits, while implementing the corresponding \mathbf{P}_k in the direct encoding uses $O(n \log(n))$ non-Clifford gate depth and $O(n)$ ancilla qubits [37].

Appendix E: Membership functions

In this section, we give an explicit construction for the membership functions \mathbf{P}_k in the case where \mathcal{K} is a clique complex and $|\sigma_k\rangle$ is represented by the compact encoding. This is an adaptation of the analogous clique-finding function given by Berry et al. [39], which applies for basis states in the direct encoding scheme (their clique-finding function is itself based on a similar algorithm by Metwalli, Le Gall, and van Meter [70]).

In general, for an arbitrary basis state $|q_0\rangle |q_1\rangle \dots |q_k\rangle$ of the system register containing $|\mathbf{s}^k\rangle$, we want to construct an operator that flags whether the following properties hold:

- (a) $0 < q_0 < q_1 < \dots < q_k$,
- (b) $\{v_{q_0}, \dots, v_{q_k}\}$ is a simplex in \mathcal{K} .

To check property (a), inequality check the register $|q_0\rangle$ against a $\lceil \log(n+1) \rceil$ -qubit ancilla register in state $|\bar{0}\rangle := |00\dots 0\rangle$. Then perform k inequality checks between neighbouring registers i and $i+1$ for $i \in \{0, \dots, k-1\}$ (that is, checking that $q_0 < q_1 < \dots < q_k$). Property (a) is satisfied if and only if $q_0 > 0$, and all other inequality checks are satisfied. This is sufficient for C_{Π_k} NOT. For $C_{\Pi'_k}$ NOT, we also need to check that $|q_{k+1}\rangle = |\bar{0}\rangle$. This can be done by

performing another equality check with the ancilla register mentioned above. Each of these checks requires a circuit of depth and Toffoli count $O(\log k)$ as well as one ancilla per check, along with a final flag qubit (using the inequality check described in Section 4.3 of Ref. [83]). The checks can be parallelised such that there are exactly two rounds of checks, and thus the depth is $O(\log k)$ with $k + 1$ ancillas and a flag qubit for passing the check.

Checking whether $\{v_{q_0}, \dots, v_{q_k}\}$ corresponds to a k -simplex is more difficult. For an arbitrary simplicial complex \mathcal{K} , it is not known if there is an efficient quantum implementation of the membership function

$$|x\rangle |0\rangle \mapsto |x\rangle |\mathbb{1}\{x \in \mathcal{K}\}\rangle,$$

where $|x\rangle$ is some basis state representing a subset of the vertex set \mathcal{V} (in compact, direct, or other encodings). If \mathcal{K} is a clique complex and $|x\rangle$ is a basis state in the direct encoding, then Berry et al. [39] give an implementation, based on work by Refs. [36, 70], of a function that implements

$$|x\rangle |0\rangle |0\rangle \mapsto |x\rangle |\mathbb{1}\{x \in \mathcal{K}\}\rangle |\text{garb}(x)\rangle,$$

where $\text{garb}(x)$ represents ancilla registers that are entangled with $|x\rangle$. This implementation requires $O(E)$ Toffolis, where $E \leq \binom{n}{2}$ is the number of edges in the underlying graph $G = (\mathcal{V}, \mathcal{E})$.

Here we adapt this circuit to the compact encoding scheme. Our circuit has depth and Toffoli count $O(Ek^2 \log n)$. The main cause for the increase in complexity is that, in the compact encoding, the location of the register containing any particular integer $j \leq n$ is not fixed. As a toy example, consider the representation of the simplices $\{v_1, v_3, v_4\}$ and $\{v_1, v_4, v_5\}$ in each encoding. In the direct encoding, these simplices are represented by the states $|10110\rangle$ and $|10011\rangle$ (assuming $n = 5$). Notably, the same qubit is used to denote the presence or absence of a particular vertex v_i in each state. On the other hand, in the compact encoding, these two simplices would be represented by the states $|001\rangle |011\rangle |100\rangle$ and $|001\rangle |100\rangle |101\rangle$. Both simplices contain vertex v_4 , but the register containing this information is different for each basis state. This means that checking for the existence of edges between vertices in a simplex requires checking between each pair of vertices in all pairs of registers. This increases the circuit complexity considerably.

The broad idea is as follows. We first define an edge-checking sub-circuit C_{ij} that acts on two registers each of size $\lceil \log(n + 1) \rceil$ (e.g. $|q_i\rangle$ and $|q_j\rangle$) and an ancilla qubit initially in state $|0\rangle$. This circuit consists of E different $(2^{\lceil \log(n + 1) \rceil})$ -controlled NOT gates, which check whether $|q_i\rangle |q_j\rangle = |a\rangle |b\rangle$ for each $v_a v_b \in \mathcal{E}$. The circuit C is then implemented across each pair of registers (i, j) where $0 \leq i < j \leq k$. If $v_{q_i} v_{q_j} \in \mathcal{E}$, then the edge checking block C_{ij} flips the ancilla. This in turn controls an increment block on another register of $2^{\lceil \log(k + 1) \rceil}$ ancillas. We perform the edge check C_{ij} again to reset the ancilla, and then do the same thing with the next edge-checking block. After all C_{ij} blocks have been run, the ancilla register is in its original state, and the incrementing register contains a binary representation of the number of edges between $\{v_{q_0}, \dots, v_{q_k}\}$ in G . Finally, we perform an equality check between this result of this register and an ancilla register containing the value $\binom{k+1}{2}$; the result of this is stored in a flag qubit initially set to $|0\rangle$. This qubit is in state $|1\rangle$ if and only if $\{v_{q_0}, \dots, v_{q_k}\}$ form a clique in G . The rest of the circuit can be then uncomputed by performing the operations in reverse. A high-level circuit diagram of this is given in Figure 7.

Each $2^{\lceil \log(n + 1) \rceil}$ -controlled NOT gate in C can be implemented in $O(\log n)$ Toffoli gates, and thus the depth and Toffoli of each block C is $O(E \log n)$. There are $\binom{k+1}{2}$ pairs of registers, and thus C must be implemented $2^{\binom{k+1}{2}}$ times to account for uncomputation of the ancilla. An increment block on $2^{\lceil \log(k + 1) \rceil}$ qubits can be implemented in $O(\log k)$ Toffoli-or-smaller gates with a single ancilla [70]. This also needs to be implemented $\binom{k+1}{2}$ times. After this, the value of this register is checked against a register containing the value $\binom{k+1}{2}$. This equality checking can be done as two different inequality checks as outlined in Section 4.3 of Ref. [83], which each use one ancilla and $O(\log k)$ gates. The output of these two inequality checks (stored in the ancillas) is then added onto the flag qubit using a 00-controlled Toffoli gate. The values in the ancillas are all uncomputed by reversing the circuit. Thus, the total depth of the clique-checking circuit is $O(Ek^2 \log n)$, as is the total number of Toffoli gates required, and there are $O(\log k)$ ancillas used.

Finally, we apply a single Toffoli gate to the flag qubits for checking properties (a) and (b). The overall action of this is

$$|x\rangle |0\rangle^{\otimes a} |0\rangle \mapsto |x\rangle |0\rangle^{\otimes a} |\mathbb{1}\{x \in \mathcal{K}\}\rangle$$

as required, for some $a \in O(k)$. Thus, the depth and Toffoli count of \mathbf{P}_k in the compact encoding is $O(Ek^2 \log n)$, since the cost of checking property (a) is comparably negligible.

We note that the depth of this circuit can be reduced by increasing the number of ancillas used in edge-checking by $k/2$. This allows us to parallelise many of the C_{ij} applications and check for the existence of all pairs of edges in either k or $k + 1$ rounds (depending on the parity of k), rather than $\binom{k+1}{2}$. In this case, each increment block is controlled

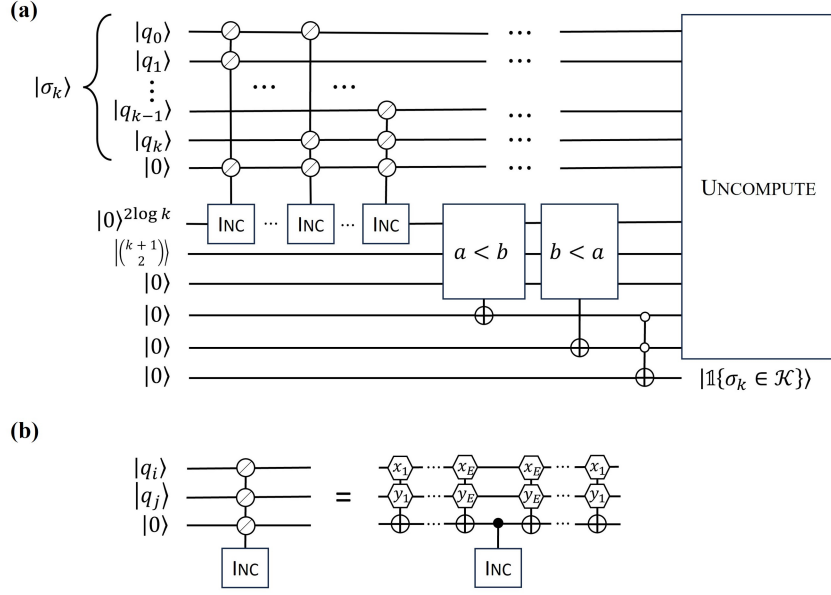


Figure 7. (a) The circuit that implements \mathbf{P}_k which maps $|\sigma_k\rangle |0\rangle \mapsto |\sigma_k\rangle |1\{\sigma_k \in \mathcal{K}\}\rangle$, where $|\sigma_k\rangle$ is a basis state satisfying property (a) and q_i is the binary representation of vertex v_{q_i} . The \otimes notation is described in the following part. (b) The edge-checking circuit C checking for the existence of an edge between vertices q_i and q_j . The \otimes is shorthand for a sequence of multi-controlled CNOT operations, described in more detail on the right-hand side. The pairs $x_i < y_i$ form a list of all edges in G . A number i inscribed in a hexagon indicates that this operation is controlled on that register containing i in binary.

by every ancilla, and the final value of this register is compared against k (or $k + 1$ depending on parity), instead of $\binom{k+1}{2}$. In this case the ancilla register containing the increment blocks does not count the number of edges between $\{v_{q_0}, \dots, v_{q_k}\}$ in G , instead grouping edges together and counting whether all the blocks have the correct number of edges in them. In this case the number of ancillas increases by approximately $k/2 - 2 \log(k+1)$, the number of Toffoli gates remains similar, and the depth changes to $O(Ek \log n)$ (the depth for checking property (a) is still negligible).

Appendix F: Proof of Lemma 1

Proof. Let $\mathbf{U}_{\mathbf{A}_i}, \Pi'_i, \Pi_i$ be as in Definition 2 for all $i \in [m]$. Theorem 5 and Corollary 1 guarantee that there exist $2m$ sequences of phase factors $\{\Phi_{g_i}, \Phi_{h_i}\}_{i \in [m]}$ and the corresponding complex-valued polynomials $\{g_i, h_i\}_{i \in [m]}$ such that

$$\Re(g_i)(\mathbf{A}_i) := g_{\Re, i}(\mathbf{A}_i) = \left(\langle + | \otimes \left(\langle 0 |^{\otimes a} \otimes \mathbf{I}^s \right) \right) \mathbf{W}_{g_{\Re, i}} \left(|+\rangle \otimes \left(|0\rangle^{\otimes a} \otimes \mathbf{I}^s \right) \right), \quad (\text{F1})$$

$$\Im(h_i)(\mathbf{A}_i) := h_{\Im, i}(\mathbf{A}_i) = \left(\langle + | \otimes \left(\langle 0 |^{\otimes a} \otimes \mathbf{I}^s \right) \right) \mathbf{W}_{h_{\Im, i}} \left(|+\rangle \otimes \left(|0\rangle^{\otimes a} \otimes \mathbf{I}^s \right) \right), \quad (\text{F2})$$

where the SELECT operations $\mathbf{W}_{g_{\Re, i}}$ and $\mathbf{W}_{h_{\Im, i}}$ are given by

$$\mathbf{W}_{g_{\Re, i}} := |0\rangle\langle 0| \otimes \Pi'_i \mathbf{U}_{\mathbf{A}_i}^{\Phi_{g_i}} \Pi_i + |1\rangle\langle 1| \otimes \Pi'_i \mathbf{U}_{\mathbf{A}_i}^{-\Phi_{g_i}} \Pi_i, \quad (\text{F3})$$

$$\mathbf{W}_{h_{\Im, i}} := \left(\mathbf{Z} \otimes \mathbf{I}^{a+s+1} \right) \left(|0\rangle\langle 0| \otimes \Pi'_i \mathbf{U}_{\mathbf{A}_i}^{\Phi_{h_i}} \Pi_i + |1\rangle\langle 1| \otimes \Pi'_i \mathbf{U}_{\mathbf{A}_i}^{-\Phi_{h_i}} \Pi_i \right). \quad (\text{F4})$$

Then, we define a new SELECT operation \mathbf{W}_f as

$$\mathbf{W}_f := \sum_{i=0}^{m-1} |i\rangle\langle i| \otimes \left(|0\rangle\langle 0| \otimes \mathbf{W}_{g_{\Re, i}} + |1\rangle\langle 1| \otimes \mathbf{W}_{h_{\Im, i}} \right) + \left(\mathbf{I}^b - |i\rangle\langle i| \right) \otimes \mathbf{I} \otimes \mathbf{I}^{a+s+2}, \quad (\text{F5})$$

where $|i\rangle\langle i|$ and $\mathbf{I}^b - |i\rangle\langle i|$ are acting on a $b = \lceil \log(2m) \rceil$ -qubit ancilla register. The overall SELECT operation \mathbf{W}_f requires $(a + b + 3)$ ancilla qubits. Let \mathbf{G} be a PREPARE operation as defined in Eq. (A1), acting on the b -qubit

register, and recall that $\beta = \|c\|_1$. Then

$$\begin{aligned} \beta \left(\langle \mathbf{G} | \otimes \langle 0 |^{\otimes(a+3)} \otimes \mathbf{I}^s \right) \mathbf{W}_f \left(| \mathbf{G} \rangle \otimes | 0 \rangle^{\otimes(a+3)} \otimes \mathbf{I}^s \right) &= \sum_{i=0}^{m-1} c_i \left(g_{\mathfrak{R},i}(\mathbf{A}_i) + i h_{\mathfrak{S},i}(\mathbf{A}_i) \right) \\ &= \sum_{i=0}^{m-1} c_i f(\mathbf{A}_i), \end{aligned}$$

proving that $\left(\langle \mathbf{G} | \otimes \langle 0 |^{\otimes(a+3)} \otimes \mathbf{I}^s \right) \mathbf{W}_f \left(| \mathbf{G} \rangle \otimes | 0 \rangle^{\otimes(a+3)} \otimes \mathbf{I}^s \right)$ is $(\beta, a + \lceil \log(2m) \rceil + 3, 0)$ -PUE of $\sum_{i=0}^{m-1} c_i f_i(\mathbf{A}_i)$.

Now we prove the second claim in the theorem. Given a $\delta > 0$ and $O(m \text{ poly}(d, 1/\delta))$ classical computation time, one can find $2m$ sequences of phase factors $\{\Phi'_{g_i}, \Phi'_{h_i}\}$ and the corresponding complex-valued polynomials $\{\text{Poly}_{g_i}^{(\text{SV})}, \text{Poly}_{h_i}^{(\text{SV})}\}$ for all $i \in [m]$, such that $\Re\left(\text{Poly}_{g_i}^{(\text{SV})}\right) = \text{Poly}_{g_{\mathfrak{R},i}}^{(\text{SV})}$ and $i\Im\left(\text{Poly}_{h_i}^{(\text{SV})}\right) = \text{Poly}_{ih_{\mathfrak{S},i}}^{(\text{SV})}$ satisfy

$$\begin{aligned} \left\| g_{\mathfrak{R},i}(\mathbf{A}_i) - \text{Poly}_{g_{\mathfrak{R},i}}^{(\text{SV})}(\mathbf{A}_i) \right\| &\leq \frac{\delta}{2}, \\ \left\| i h_{\mathfrak{S},i}(\mathbf{A}_i) - \text{Poly}_{ih_{\mathfrak{S},i}}^{(\text{SV})}(\mathbf{A}_i) \right\| &\leq \frac{\delta}{2}, \end{aligned}$$

and thus

$$\left\| f_i(\mathbf{A}_i) - \left(\text{Poly}_{g_{\mathfrak{R},i}}^{(\text{SV})}(\mathbf{A}_i) + \text{Poly}_{ih_{\mathfrak{S},i}}^{(\text{SV})}(\mathbf{A}_i) \right) \right\| \leq \frac{\delta}{2} + \frac{\delta}{2} := \delta.$$

Here, we change $\mathbf{U}_{\mathbf{A}_i}^{\Phi_{g_i}}$ and $\mathbf{U}_{\mathbf{A}_i}^{\Phi_{h_i}}$ in Eqs. (F3) and (F4) to $\mathbf{U}_{\mathbf{A}_i}^{\Phi'_{g_i}}$ and $\mathbf{U}_{\mathbf{A}_i}^{\Phi'_{h_i}}$, and in turn define the corresponding SELECT operation $\mathbf{W}_{f'}$ analogously to \mathbf{W}_f in Eq. (F5) to build $\text{Poly}_{g_{\mathfrak{R},i}}^{(\text{SV})}(\mathbf{A}_i)$ and $\text{Poly}_{ih_{\mathfrak{S},i}}^{(\text{SV})}(\mathbf{A}_i)$ for all $i \in [m]$. Thus,

$$\begin{aligned} &\left\| \sum_{i=0}^{m-1} c_i f(\mathbf{A}_i) - \beta \left(\langle \mathbf{G} | \otimes \langle 0 |^{\otimes(a+3)} \otimes \mathbf{I}^s \right) \mathbf{W}_f \left(| \mathbf{G} \rangle \otimes | 0 \rangle^{\otimes(a+3)} \otimes \mathbf{I}^s \right) \right\| \\ &= \left\| \sum_{i=0}^{m-1} c_i f(\mathbf{A}_i) - c_i \left(\text{Poly}_{g_{\mathfrak{R},i}}^{(\text{SV})}(\mathbf{A}_i) + \text{Poly}_{ih_{\mathfrak{S},i}}^{(\text{SV})}(\mathbf{A}_i) \right) \right\| \\ &\leq \sum_{i=0}^{m-1} c_i \left\| f(\mathbf{A}_i) - \left(\text{Poly}_{g_{\mathfrak{R},i}}^{(\text{SV})}(\mathbf{A}_i) + \text{Poly}_{ih_{\mathfrak{S},i}}^{(\text{SV})}(\mathbf{A}_i) \right) \right\| \\ &\leq \sum_{i=0}^{m-1} c_i \delta = \beta \delta, \end{aligned}$$

proving that $\left(\langle \mathbf{G} | \otimes \langle 0 |^{\otimes(a+3)} \otimes \mathbf{I}^s \right) \mathbf{W}_f \left(| \mathbf{G} \rangle \otimes | 0 \rangle^{\otimes(a+3)} \otimes \mathbf{I}^s \right)$ is $(\beta, a + \lceil \log(2m) \rceil + 3, \beta\delta)$ -PUE of $\sum_{i=0}^{m-1} c_i f_i(\mathbf{A}_i)$. \square

Appendix G: Proof of Lemma 2

Proof. As described in Section IV B, there exists a $(\alpha_k, a_k, 0)$ -PUE of \mathbf{B}_k and a $(\alpha_{k+1}, a_{k+1}, 0)$ -PUE of \mathbf{B}_{k+1} . We make use of Lemma 1 to create a linear combination of two even polynomials of \mathcal{B}_k and $\mathcal{B}_{k+1}^\dagger$ and an identity map. Define $f : [-1, 1] \rightarrow [0, 1]$ such that $f(x) = x^2$. Given g^G, g^C as defined by their polynomial coefficients $\{\mathfrak{h}_0, \mathfrak{h}_{i_\ell}^\ell, \mathfrak{h}_{i_u}^u\}$, we define two even polynomials $h^G := g^G \circ f$ and $h^C := g^C \circ f$. Since $g^G, g^C : [0, 1] \rightarrow [-1, 1]$, it follows that $h^G, h^C : [-1, 1] \rightarrow [0, 1]$. Thus, Corollary 1 implies that there exist two sequences of phase factors $\Phi_\ell \in \mathbb{R}^{2d_\ell}, \Phi_u \in \mathbb{R}^{2d_u}$ and the corresponding alternating phased sequences $\mathbf{U}_{\mathbf{B}_k}^{\Phi_\ell}, \mathbf{U}_{\mathbf{B}_{k+1}^\dagger}^{\Phi_u}$ (these terms are defined explicitly in Appendices A and B) which construct $h^G(\mathcal{B}_k) = g^G(\mathcal{L}_k^\ell)$ and $h^C(\mathcal{B}_{k+1}^\dagger) = g^C(\mathcal{L}_k^u)$. Applying the construction in Lemma 1 with $c_0 = \mathfrak{h}_0$ and $c_1 = c_2 = 1$ gives a $(\beta, a_k + a_{k+1} + a_p + 6, 0)$ -PUE of $H^{(\text{SV})}(\mathcal{L}_k^\ell, \mathcal{L}_k^u)$, where $\beta = \|c\|_1 = \mathfrak{h}_0 + 2$.

To calculate the precise cost, we see from Theorem 5 that implementing $\mathbf{U}_{\mathbf{B}_k}^{\Phi_\ell}$, $\mathbf{U}_{\mathbf{B}_{k+1}}^{\Phi_u}$, $\mathbf{U}_{\mathbf{B}_k}^{-\Phi_\ell}$, and $\mathbf{U}_{\mathbf{B}_{k+1}}^{-\Phi_u}$ requires $4d_\ell$ calls to $\mathbf{U}_{\mathbf{B}_k}$, $\mathbf{U}_{\mathbf{B}_k}^\dagger$ and $4d_u$ calls to $\mathbf{U}_{\mathbf{B}_{k+1}}$, $\mathbf{U}_{\mathbf{B}_{k+1}}^\dagger$ respectively, with $8d_\ell$ calls of $\mathbf{C}_{\Pi_{k-1}} \mathbf{NOT}$, $\mathbf{C}_{\Pi_k} \mathbf{NOT}$ and $8d_u$ calls to $\mathbf{C}_{\Pi'_k} \mathbf{NOT}$, $\mathbf{C}_{\Pi_{k+1}} \mathbf{NOT}$. Furthermore, Lemma 1 implies that we require $a = a_k + a_{k+1} + a_p$ ancilla qubits for constructing $\mathbf{U}_{\mathbf{B}_k}^{\Phi_\ell}$ and $\mathbf{U}_{\mathbf{B}_{k+1}}^{\Phi_u}$ (recall that a_p is the ancilla qubits used in the membership function \mathbf{P}_k), $b = 2$ ancilla qubits for the PREPARE operation, and two ancilla qubits for constructing the real-valued polynomials. There are two additional qubits introduced because we differentiate the ancilla used in $\mathbf{U}_{\mathbf{B}_k}$ and $\mathbf{U}_{\mathbf{B}_{k+1}}^\dagger$. \square

Remark 1. As described in Lemma 1, given $\delta > 0$ and using $O(\text{poly}(d, \log(1/\delta)))$ classical computation time one can obtain two sequences of phase factors $\Phi'_\ell \in \mathbb{R}^{2d_\ell}$, $\Phi'_u \in \mathbb{R}^{2d_u}$, and the corresponding alternating phased sequences $\mathbf{U}_{\mathbf{B}_k}^{\Phi'_\ell}$ and $\mathbf{U}_{\mathbf{B}_{k+1}}^{\Phi'_u}$, which construct polynomials $\text{Poly}_{h^G}^{(\text{SV})}(\mathbf{B}_k)$, $\text{Poly}_{h^C}^{(\text{SV})}(\mathbf{B}_{k+1}^\dagger)$ of degree $2d_\ell$ and $2d_u$ respectively such that

$$\left\| h^G(\mathbf{B}_k) - \text{Poly}_{h^G}^{(\text{SV})}(\mathbf{B}_k) \right\| \leq \delta/2 \quad \text{and} \quad \left\| h^C(\mathbf{B}_{k+1}^\dagger) - \text{Poly}_{h^C}^{(\text{SV})}(\mathbf{B}_{k+1}^\dagger) \right\| \leq \delta/2.$$

Implementing the LCU method as in Lemma 1, we obtain

$$\left\| H_d^{(\text{SV})}(\mathcal{L}_k^\ell, \mathcal{L}_k^u) - \beta \left(\text{Poly}_{h^G}^{(\text{SV})}(\mathbf{B}_k) + \text{Poly}_{h^C}^{(\text{SV})}(\mathbf{B}_{k+1}^\dagger) - \mathfrak{h}_0 \mathbf{I} \right) \right\| \leq \beta\delta,$$

which gives a $\beta\delta$ -approximation to $H_d^{(\text{SV})}/\beta$.

Appendix H: Proof of Lemma 3

Proof. We focus our calculation on approximating the gradient projector, as the calculation for the curl projector is analogous. Let $\varepsilon'_\ell = \frac{\alpha_k^2 \varepsilon_\ell}{n}$ and $\varepsilon'_u = \frac{\alpha_{k+1}^2 \varepsilon_u}{n}$, where $\varepsilon_\ell, \varepsilon_u \in (0, 1/2)$. Recall that $\kappa_\ell := \kappa_{\text{eff}}(\mathbf{B}_k)$ and $\kappa_u := \kappa_{\text{eff}}(\mathbf{B}_{k+1})$ are the effective condition numbers of \mathbf{B}_k and \mathbf{B}_{k+1} respectively. Thus, the condition numbers of \mathbf{L}_k^ℓ and \mathbf{L}_k^u are κ_ℓ^2 and κ_u^2 respectively. Theorem 41 of Ref. [44] states that there exists a real degree- d polynomial $g_d : [-1, 1] \rightarrow [-1, 1]$ that $\frac{\varepsilon'}{2\kappa}$ -approximates the function $\frac{1}{2\kappa x}$ for all $x \in [-1, 1] \setminus [-\frac{1}{\kappa}, \frac{1}{\kappa}]$ such that $|g_d(x)| \leq 1$ for all $x \in [-1, 1]$, $g_d(0) = 0$, and $d = O(\kappa \log(\kappa/\varepsilon'))$. For approximating the gradient projector, we set $\kappa := \kappa_\ell^2$ and $\varepsilon' := \varepsilon'_\ell$, (naturally setting $\kappa := \kappa_u^2$ and $\varepsilon' := \varepsilon'_u$, and adjusting d accordingly when approximating the curl projector). Note that the nonzero spectra of \mathbf{L}_k^ℓ and \mathbf{L}_{k-1}^u are the same [68], and so their condition numbers are equal.

Now consider the function $H_{d+1}(x) = x^2 g_d(x^2)$, defined on $[-1, 1]$. The aforementioned properties of $g_d(x)$ imply that

$$\sup_{|x| \leq 1} |H_{d+1}(x)| = \sup_{|x| \leq 1} |x^2 g_d(x^2)| \leq \sup_{|x| \leq 1} |g_d(x^2)| \leq 1.$$

If $g_d(x)$ is a degree- d polynomial of x^2 then $H_{d+1}(x)$ is a degree- $(d+1)$ polynomial of x^2 (equivalently a degree- $(2d+2)$ polynomial of x). Suppose that $g_d(x) = \sum_{i=0}^d c_i x^i$ for some real constants c_i . We also suppose that the singular value decomposition of \mathbf{B}_k is given by $\mathbf{B}_k = \sum_j \sigma_j |\tilde{\psi}_j\rangle \langle \psi_j|$ where $\sigma_j \geq 0$. It follows that $\mathbf{L}_{k-1}^u = \mathbf{B}_k \mathbf{B}_k^\dagger = \sum_j \lambda_j |\tilde{\psi}_j\rangle \langle \tilde{\psi}_j|$ where $\lambda_j = \sigma_j^2$. This implies that

$$\begin{aligned} H_{d+1}^{(\text{SV})} \left(\frac{\mathbf{L}_k^\ell}{\alpha_k^2} \right) &= \frac{1}{\alpha_k^2} \mathbf{B}_k^\dagger \mathbf{B}_k g_d^{(\text{SV})} \left(\frac{\mathbf{B}_k^\dagger \mathbf{B}_k}{\alpha_k^2} \right) = \frac{1}{\alpha_k^2} \mathbf{B}_k^\dagger \mathbf{B}_k \left(\sum_{i=0}^d c_i \left(\frac{\mathbf{B}_k^\dagger \mathbf{B}_k}{\alpha_k^2} \right)^i \right) = \frac{1}{\alpha_k^2} \mathbf{B}_k^\dagger \left(\sum_{i=0}^d c_i \left(\frac{\mathbf{B}_k \mathbf{B}_k^\dagger}{\alpha_k^2} \right)^i \right) \mathbf{B}_k \\ &= \frac{1}{\alpha_k^2} \mathbf{B}_k^\dagger \left(\sum_{i=0}^d c_i \left(\frac{\mathbf{L}_{k-1}^u}{\alpha_k^2} \right)^i \right) \mathbf{B}_k = \frac{1}{\alpha_k^2} \mathbf{B}_k^\dagger \frac{\alpha_k^2}{2\kappa_k^2} (\mathbf{L}_{k-1}^u)^+ \mathbf{B}_k + \frac{1}{\alpha_k^2} \mathbf{B}_k^\dagger \sum_j \delta'_j |\tilde{\psi}_j\rangle \langle \tilde{\psi}_j| \mathbf{B}_k \end{aligned}$$

where $\delta'_j \in \left[-\frac{\varepsilon'_\ell}{2\kappa_\ell^2}, \frac{\varepsilon'_\ell}{2\kappa_\ell^2} \right]$. Thus,

$$H_{d+1}^{(\text{SV})} \left(\frac{\mathbf{L}_k^\ell}{\alpha_k^2} \right) = \frac{1}{2\kappa_\ell^2} \mathbf{B}_k^\dagger (\mathbf{L}_{k-1}^u)^+ \mathbf{B}_k + \mathbf{B}_k^\dagger \left(\sum_j \delta_j |\tilde{\psi}_j\rangle \langle \tilde{\psi}_j| \right) \mathbf{B}_k = \frac{1}{2\kappa_\ell^2} \mathbf{B}_k^\dagger (\mathbf{L}_{k-1}^u)^+ \mathbf{B}_k + \sum_j \lambda_j \delta_j |\psi_j\rangle \langle \psi_j|,$$

for $\delta \in \left[-\frac{\varepsilon_\ell}{2n\kappa_\ell^2}, \frac{\varepsilon_\ell}{2n\kappa_\ell^2}\right]$. It is shown in Ref. [84] that $\lambda_i \leq n$ for all i . Recall that $\mathbf{B}_k = \mathbf{B}_k/\alpha_k$. Thus,

$$\left\| \Pi^G - 2\kappa_\ell^2 H_{d+1}^{(SV)} \left(\frac{\mathbf{L}_k^\ell}{\alpha_k^2} \right) \right\| = \left\| 2\kappa_\ell^2 \sum_j \lambda_j \delta_j |\psi_j\rangle \langle \psi_j| \right\| \leq \left\| 2\kappa_\ell^2 \sum_j \frac{\varepsilon_\ell}{2\kappa_\ell^2} |\psi_j\rangle \langle \psi_j| \right\| \leq \varepsilon_\ell.$$

Note that H_{d+1} is a polynomial of degree $2d+2$ where $d = O(\kappa_\ell^2 \log((n\kappa_\ell)^2/(\alpha_\ell^2 \varepsilon_\ell)))$. This completes the proof of the approximation of the gradient projector; as mentioned above, the approximation of the curl projector is analogous. \square

Remark 2. We can also define $H'_{d+1}(x) = xg_d(x^2)$. This approximates a modified projector $\Pi^{G'}$ with the action

$$\Pi^{G'} \mathbf{s}^k = \mathbf{s}^{k-1}$$

where \mathbf{s}^{k-1} is the (minimum Euclidean norm) vector such that $\mathbf{B}_k^T \mathbf{s}^{k-1} = \mathbf{s}^k$. The function $H'_{d+1}(x)$ is a degree- $(2d+1)$ polynomial that also satisfies $|H'_{d+1}(x)| \leq 1$ for all $x \in [-1, 1]$. Performing a similar calculation to above, it follows that there exists some $d \in O(\kappa_\ell^2 \log(n\kappa_\ell^2/(\alpha_k \varepsilon_\ell)))$ such that $\|\Pi^{G'} - 2\frac{\kappa_\ell^2}{\alpha_k} H'_{d+1}\| \leq \varepsilon$.